

Up-Regulation of Cluster of Differentiation (CD) 11b Expression on the Surface of Canine Granulocytes with Human Granulocyte-Macrophage Colony-Stimulating Factor (GM-CSF)

Kazuhide NAKAGAKI^{1)*}, Yuka NUNOMURA¹⁾, Kanji UCHIDA²⁾, Koh NAKATA³⁾ and Ryushi TAZAWA³⁾

¹⁾Department of Virology and Immunology, College of Veterinary Medicine, Nippon Veterinary and Animal Science University, Tokyo 180-8602, Japan

²⁾Department of Anesthesiology, the University of Tokyo Hospital, Tokyo 113-0033, Japan

³⁾Bioscience Medical Research Center, Niigata University Medical and Dental Hospital, Niigata 951-8520, Japan

(Received 29 January 2014/Accepted 25 April 2014/Published online in J-STAGE 15 May 2014)

ABSTRACT. Granulocyte-macrophage colony-stimulating factor (GM-CSF) is a pleiotropic cytokine, sharing a common beta subunit (CDw131) with interleukins 3 and 5. GM-CSF is important for its direct and indirect involvement in host defense. In veterinary medicine, human (h) GM-CSF has been used as a substitute for canine GM-CSF to stimulate canine granulocytes and macrophages. In this study, we compared the effects of three distinct hGM-CSFs produced by bacteria, yeasts and Chinese hamster ovary (CHO) cells with those of *Escherichia* (*E. coli*)-produced canine GM-CSF on the cluster of differentiation 11b (CD11b) expression in canine granulocytes. The median effective dose (ED₅₀) of hGM-CSFs from bacteria, yeasts and CHO cells was 3.09, 4.09 and 4.27 ng/ml, respectively, with no significant difference among three. In contrast, a significant difference was observed between ED₅₀ of canine GM-CSF (0.56 ng/ml) and three hGM-CSFs according to the paired *t*-test ($P < 0.05$). We conclude that hGM-CSF can activate canine granulocytes, but the average activity of the three rhGM-CSFs was approximately 15% of that of canine GM-CSF.

KEY WORDS: canine, CD11b, flow cytometry, granulocyte-macrophage colony-stimulating factor, median fluorescence intensity, xenostimulation
doi: 10.1292/jvms.14-0056; *J. Vet. Med. Sci.* 76(8): 1173–1176, 2014

Human granulocyte-macrophage colony-stimulating factor (hGM-CSF) is a protein of 144 amino acids (AA), including the signal peptide of 18 AA, and is produced by various types of cells. The protein is monomeric, but its active form basically takes a noncovalent homodimer in nature. Although GM-CSF is a major cytokine for hemopoiesis like granulocyte colony-stimulating factor, macrophage colony-stimulating factor and erythropoietin, the cytokine has been known to be involved in the enhancement of eosinophil chemotaxis [7], maturation of macrophages and dendritic cells [17], granulocyte activation [1], adjuvant effect [3] and inhibition of apoptosis [4].

Cluster of differentiation molecule 11b (CD11b), known as its integrin α M subunit, consists of macrophage-1 antigen (Mac-1) with CD18. The molecule is expressed in many types of cells, and the CD11b expression on the surfaces of granulocytes and macrophages is increased by their activation, playing an important role in host defense. Mac-1 has been reported to support neutrophil immobilization and migration [6] and is also known as complement receptor 3 (CR3) that binds to iC3b, eliminating pathogens and

immune complexes by neutrophils, macrophages and the reticuloendothelial system. CD11b is rapidly elevated by the activation of neutrophils and macrophages, and the amount of CD11b in neutrophils correlates with their activation and inflammation [11].

Clinical trials of the adjuvant therapy and the prevention form leukocytopenia with GM-CSF in veterinary cancer medicine have been started, but the preparation of canine GM-CSF for clinical use is still unavailable. Thus, we just have to choose that of human GM-CSF (hGM-CSF) at the present time. Because hGM-CSF is active in canine cells, it has been empirically employed as a substitute for canine GM-CSF [18, 22]; however, its quantitative activity in canine cells has not been elucidated. Here, we compared the effects of hGM-CSF to those of canine GM-CSF in canine granulocytes and also measured the median effective doses (ED₅₀) of three different rhGM-CSFs in canine granulocytes.

Anti-CD11b (M1/70) conjugated with allophycocyanin-Cy7, Gr-1 with allophycocyanin and anti-human CD14 with phycoerythrin were purchased from BioLegend Co., Ltd. (San Diego, CA, U.S.A.; provided by Tomy Digital, Tokyo, Japan). Molgramostim; *Escherichia* (*E. coli*)-produced recombinant human GM-CSF (rhGM-CSF), sargramostim produced by yeasts and canine recombinant GM-CSF were obtained from Amoytop Biotech (Xiamen, Fujian, People's Republic of China), Genzyme corporation (Cambridge, MA, U.S.A.) and R&D systems (Minneapolis, MN, U.S.A.), respectively. JCR Pharmaceuticals Co., Ltd. (Akashi, Japan) donated rhGM-CSF produced by Chinese hamster ovary (CHO) cells.

*CORRESPONDENCE TO: NAKAGAKI, K., Department of Virology and Immunology, College of Veterinary Medicine, Nippon Veterinary and Animal Science University, 1-7-1 Kyonan, Musashino, Tokyo 180-8602, Japan. e-mail: kazu_nakagaki@hotmail.com

©2014 The Japanese Society of Veterinary Science

This is an open-access article distributed under the terms of the Creative Commons Attribution Non-Commercial No Derivatives (by-nc-nd) License <<http://creativecommons.org/licenses/by-nc-nd/3.0/>>.

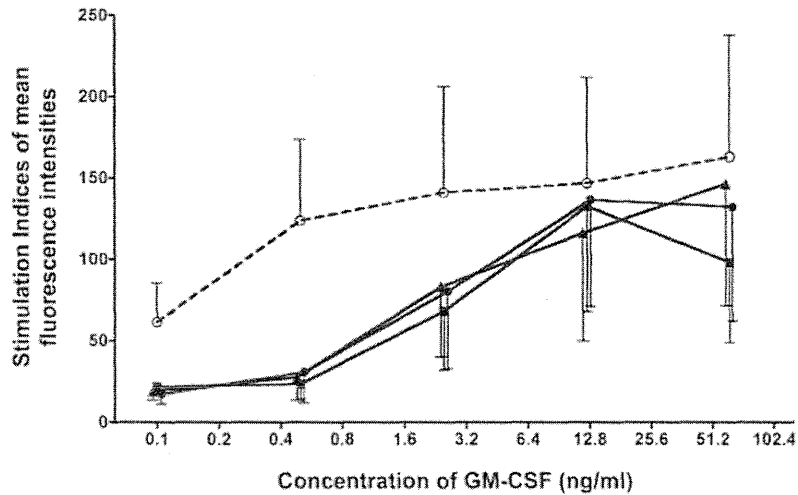


Fig. 1. Dose-response curves of CD11b expression with various granulocyte-macrophage colony-stimulating factors in canine granulocytes. Sigmoid curves represent dose-responses of molgramostim (solid circle), sargramostim (solid square), CHO-produced hGM-CSF (solid triangle) and canine GM-CSF (open circle and broken line). The points and bars show the average values and standard deviations from 4 animals, respectively. X and Y axes show the concentrations of GM-CSF (ng/ml) and stimulation indices, respectively.

Heparinized canine blood was obtained from 2 male and 2 female beagles for practical trainings of students at Nippon Veterinary and Life Science University. These beagles were individually housed, fed dog chows once a day and drank water *ad libitum*. These bloods were transported to our laboratory and processed at room temperature within 1 hr. Briefly, 100- μl aliquots of the blood were aseptically placed in 2.0-ml sterile microtubes, to which various amounts of canine or hGM-CSF were added at final concentrations of 0.02–62.5 ng/ml or macrophage-serum free medium (macrophage-SFM; Invitrogen Corporation, Carlsbad, CA, U.S.A.) alone. Subsequently, all the samples were incubated for 15 min at a 37°C in a 5% CO₂ incubator without shaking.

After stimulation, antibody cocktail was added to each tube, which was then incubated for 30 min at 4°C. The blood was hemolyzed with 0.15 M ammonium chloride containing 1 mM KHCO₃ and 0.1 mM EDTA 4Na (pH 7.3), washed twice with flow cytometer buffer (PBS containing 2% BSA and 0.1% sodium azide) and then fixed in FluoroFix™ buffer (BioLegend), as per the manufacturer's instructions. The cells were re-suspended in 100 μl flow cytometer buffer (PBS containing 2% BSA and 0.05% sodium azide). Data were acquired using FACSArray (BD Bioscience, San Jose, CA, U.S.A.), gating the granulocyte area on a forward vs. side scatter. The median fluorescence intensities (MFIs) of CD11b⁺ population were obtained under the gate of granulocytes at SSC vs. FSC scatter and CD14⁻. The indices of MFIs were determined by dividing MFIs from GM-stimulated cultures by MFI from PBS-cultured granulocytes. ED₅₀, determined from MFI values using the probit method, was statistically analyzed using paired *t*-tests at every GM-CSF dose.

Three hGM-CSFs revealed increased CD11b expression on canine granulocytes in a dose-dependent manner (Fig. 1). ED₅₀ of molgramostim, sargramostim and hGM-CSF from CHO cells was 3.09, 4.09 and 4.27 ng/ml , respectively; moreover, no significant difference was observed among these rhGM-CSFs (Table 1). In contrast, ED₅₀ of canine rGM-CSF was 0.56 ng/ml , which was significantly different from the three rhGM-CSFs according to the paired *t*-test results ($P < 0.05$). Further, ED₅₀ of molgramostim, sargramostim and rhGM-CSF from the CHO cells was 18.1%, 13.7% and 13.1%, respectively, compared with the canine rGM-CSF for canine granulocytes.

GM-CSF is not only an important hemopoietic cytokine, but also involved in the upregulation of the immune system and host-defense [5, 19, 21], because immune cells express its receptor [10, 14]. In experiments using dogs, rhGM-CSF has been employed as a substitute for the canine reagent [2, 16].

GM-CSF activity is usually measured by the proliferation of cells that are GM-CSF-dependent; e.g. TF-1 for hGM-CSF [9]. The detection of augmented CD11b with GM-CSF is rapid and easy. CD11b expression on the surface of neutrophils has been reported to elevate by GM-CSF stimulation [12, 15]. Uchida *et al.* have reported that the quick elevation of CD11b expression on human neutrophils by GM-CSF stimulation was caused by its endogenous molecules but not de novo synthesis [20]. According to a modified Uchida method [20], we detected the activities of rhGM-CSFs in canine neutrophils in a dose-dependent manner. We conclude it may not be a problem to employ rhGM-CSF to canine experiment. This technique doesn't require any GM-CSF-dependent cell line and is applicable to every animal species.

Table 1. Median effective doses of various granulocyte-macrophage colony-stimulating factors in expression of CD11b in canine granulocytes

GM-CSF	ED ₅₀ (ng/ml)	Specific activities (units/ μ g)	Relative activities (%) to canine GM-CSF in ED ₅₀
Molgramostim	3.09 \pm 1.18 ^a	323.6	18.1
Sargramostim	4.09 \pm 1.56 ^a	244.5	13.7
CHO hGM-CSF	4.27 \pm 1.51 ^a	234.2	13.1
Canine GM-CSF	0.56 \pm 0.46 ^a	1,785.7	–

a) Median effective dose (ED₅₀) of canine granulocyte-macrophage colony-stimulating factor (GM-CSF) significantly differed from those of hGM-CSFs according to the paired *t*-test results (*P*<0.05).

Furthermore, it has been reported that some mouse cells are not stimulated by hGM-CSF. However, McClure *et al.* proved that rhGM-CSF activated the BaF-B03 mouse cell line transfected with human GM-CSF receptor α subunit gene [13]. The intracytoplasmic region of the subunit did not participate in the signal transduction [23], which suggests that the α subunit plays an important role in binding species-specifically to GM-CSF. Therefore, the α subunit of canine GM-CSF may have an effective affinity to rhGM-CSF, although rhGM-CSFs had a weaker impact on canine granulocytes compared with canine rGM-CSF in this study. Therefore, to obtain an effect equivalent to an expected activity in dogs with hGM-CSF, we must employ an approximately septuplet dose of rhGM-CSF (Table 1). Nevertheless, this indicates that rhGM-CSF can be a valuable tool for a canine study.

In addition, we also compared GM-CSFs from three different sources: *E. coli*, yeasts and CHO cells; although no significant difference was determined in ED₅₀ for the three sources, *E. coli*-produced rhGM-CSF (molgramostim) revealed the highest activity. Moreover, Kelleher *et al.* determined that *E. coli*-produced hGM-CSF had higher efficacy with regard to the proliferation of TF-1 cells compared with that of CHO protein [8]. Although we are not able to explain why molgramostim exhibited the highest activity in our study, Kelleher *et al.* suggested that the difference was the result of the higher affinity of *E. coli* protein [8]. Molgramostim is not much different from the other two types investigated without their glycosylation, which may be involved in their 3-D conformation and homodimer formation and/or interfere with their interactions with GM-CSFR, affecting GM-CSF activity. Thus, the differences in glycosylation may be responsible for their varied activities.

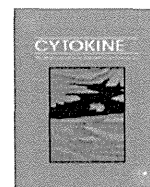
ACKNOWLEDGMENTS. We thank Ms. Natuko Nogami, a Junior Research Assistant for her technical support. Supported by a grant from the Ministry of Health Labor and Welfare, Japan (H24-Rinkensui-Ippan-003) and in part by the program for the Strategic Research Foundation at Private Universities, 2009–12 of the Japanese Ministry of Education, Culture, Sports, Science and Technology, Tokyo, Japan.

REFERENCES

1. Al-Shami, A. and Naccache, P. H. 1999. Granulocyte-macrophage colony-stimulating factor-activated signaling pathways in

- human neutrophils. Involvement of jak2 in the stimulation of phosphatidylinositol 3-kinase. *J. Biol. Chem.* **274**: 5333–5338. [Medline] [CrossRef]
2. Bergman, P. J., Camps-Palau, M. A., McKnight, J. A., Leibman, N. F., Craft, D. M., Leung, C., Liao, J., Riviere, I., Sadelain, M., Hohenhaus, A. E., Gregor, P., Houghton, A. N., Perales, M. A. and Wolchok, J. D. 2006. Development of a xenogeneic DNA vaccine program for canine malignant melanoma at the Animal Medical Center. *Vaccine* **24**: 4582–4585. [Medline] [CrossRef]
3. Chen, Q., He, F., Kwang, J., Chan, J. K. and Chen, J. 2012. GM-CSF and IL-4 stimulate antibody responses in humanized mice by promoting T, B, and dendritic cell maturation. *J. Immunol.* **189**: 5223–5229. [Medline] [CrossRef]
4. Choi, J. K., Kim, K. H., Park, H., Park, S. R. and Cho, B. H. 2011. Granulocyte-macrophage colony-stimulating factor shows anti-apoptotic activity in neural progenitor cells via JAK/STAT5-Bcl-2 pathway. *Apoptosis* **16**: 127–134. [Medline] [CrossRef]
5. Fleetwood, A. J., Cook, A. D. and Hamilton, J. A. 2005. Functions of granulocyte-macrophage colony-stimulating factor. *Crit. Rev. Immunol.* **25**: 405–428. [Medline] [CrossRef]
6. Hughes, B. J., Holler, J. C., Crockett-Torabi, E. and Smith, C. W. 1992. Recruitment of CD11b/CD18 to the neutrophil surface and adherence dependent locomotion. *J. Clin. Invest.* **90**: 1687–1696. [Medline] [CrossRef]
7. Kaatz, M., Berod, L., Czeck, W., Idzko, M., Lagadari, M., Bauer, A. and Norgauer, J. 2004. Interleukin-5, interleukin-3 and granulocyte-macrophage colony-stimulating factor prime actin-polymerization in human eosinophils: A study with hypodense and normodense eosinophils from patients with atopic dermatitis. *Int. J. Mol. Med.* **14**: 1055–1060. [Medline]
8. Kelleher, C. A., Wong, G. G., Clark, S. C., Schendel, P. F., Minden, M. D. and McCulloch, E. A. 1988. Binding of iodinated recombinant human GM-CSF to the blast cells of acute myeloblastic leukemia. *Leukemia* **2**: 211–215. [Medline]
9. Kitamura, T., Tange, T., Terasawa, T., Chiba, S., Kuwaki, T., Miyagawa, K., Piao, Y. F., Miyazono, K., Urabe, A. and Takaku, F. 1989. Establishment and characterization of a unique human cell line that proliferates dependently on GM-CSF, IL-3, or erythropoietin. *J. Cell. Physiol.* **140**: 323–334. [Medline] [CrossRef]
10. Liontos, L. M., Dissanayake, D., Ohashi, P. S., Weiss, A., Dragone, L. L. and McGlade, C. J. 2011. The Src-like adaptor protein regulates GM-CSFR signaling and monocytic dendritic cell maturation. *J. Immunol.* **186**: 1923–1933. [Medline] [CrossRef]
11. Lundahl, J., Jacobson, S. H. and Paulsson, J. M. 2012. IL-8 from local subcutaneous wounds regulates CD11b activation. *Scand. J. Immunol.* **75**: 419–425. [Medline] [CrossRef]
12. Maurer, D., Fischer, G. F., Felzmann, T., Majdic, O., Gschwantler, E., Hinterberger, W., Wagner, A. and Knapp, W. 1991. Ratio of complement receptor over Fc-receptor III expression: a sensitive parameter to monitor granulocyte-monocyte colony-stimulating

- factor effect on neutrophils. *Ann. Hematol.* **62**: 135–140. [Medline] [CrossRef]
13. McClure, B., Stomski, F., Lopez, A. and Woodcock, J. 2001. Perverted responses of the human granulocyte-macrophage colony-stimulating factor receptor in mouse cell lines due to cross-species beta-subunit association. *Blood* **98**: 3165–3168. [Medline] [CrossRef]
 14. Min, L., Mohammad Isa, S. A., Shuai, W., Piang, C. B., Nih, F. W., Kotaka, M. and Ruedl, C. 2010. Granulocyte-macrophage colony-stimulating factor is the major CD8⁺ T cell-derived licensing factor for dendritic cell activation. *J. Immunol.* **184**: 4625–4629. [Medline] [CrossRef]
 15. Neuman, E., Huleatt, J. W. and Jack, R. M. 1990. Granulocyte-macrophage colony-stimulating factor increases synthesis and expression of CR1 and CR3 by human peripheral blood neutrophils. *J. Immunol.* **145**: 3325–3332. [Medline]
 16. Nothdurft, W., Selig, C., Fliedner, T. M., Hintz-Obertreis, P., Kreja, L., Krumwieg, D., Kurrle, R., Seiler, F. R. and Weinsheimer, W. 1992. Haematological effects of rhGM-CSF in dogs exposed to total-body irradiation with a dose of 2.4 Gy. *Int. J. Radiat. Biol.* **61**: 519–531. [Medline] [CrossRef]
 17. Reddy, A., Sapp, M., Feldman, M., Subklewe, M. and Bhardwaj, N. 1997. A monocyte conditioned medium is more effective than defined cytokines in mediating the terminal maturation of human dendritic cells. *Blood* **90**: 3640–3646. [Medline]
 18. Schuening, F. G., Storb, R., Goehle, S., Nash, R., Graham, T. C., Appelbaum, F. R., Hackman, R., Sandmaier, B. M. and Urdal, D. L. 1989. Stimulation of canine hematopoiesis by recombinant human granulocyte-macrophage colony-stimulating factor. *Exp. Hematol.* **17**: 889–894. [Medline]
 19. Trapnell, B. C. and Whitsett, J. A. 2002. GM-CSF regulates pulmonary surfactant homeostasis and alveolar macrophage-mediated innate host-defense. *Annu. Rev. Physiol.* **64**: 775–802. [Medline] [CrossRef]
 20. Uchida, K., Beck, D. C., Yamamoto, T., Berclaz, P.Y., Abe, S., Staudt, M. K., Carey, B. C., Filippi, M.D., Wert, S. E., Denson, L. A., Puchalski, J. T., Hauck, D. M. and Trapnell, B. C. 2007. GM-CSF autoantibodies and neutrophil dysfunction in pulmonary alveolar proteinosis. *N. Engl. J. Med.* **356**: 567–579. [Medline] [CrossRef]
 21. Vreugdenhil, G., Preyers, F., Croockewit, S., Sauerwein, R., Swaak, A. J. and de Witte, T. 1992. Fever in neutropenic patients treated with GM-CSF representing enhanced host defence. *Lancet* **339**: 1118–1119. [Medline] [CrossRef]
 22. Wang, Y-S., Chi, K-H., Liao, K-W., Liu, C-C., Cheng, C-L., Lin, Y-C., Cheng, C-H. and Chu, R-M. 2007. Characterization of canine monocyte-derived dendritic cells with phenotypic and functional differentiation. *Can. J. Vet. Res.* **71**: 165–174. [Medline]
 23. Watanabe, S., Aoki, Y., Nishijima, I., Xu, M.J. and Arai, K. 2000. Analysis of signals and functions of the BA/F3 cells and transgenic mice colony-stimulating factor receptor in chimeric human granulocyte-macrophage. *J. Immunol.* **164**: 3635–3644. [Medline] [CrossRef]



Low concentrations of recombinant granulocyte macrophage-colony stimulating factor derived from Chinese hamster ovary cells augments long-term bioactivity with delayed clearance *in vitro*

Atsushi Hashimoto^a, Takahiro Tanaka^a, Yuko Itoh^a, Akira Yamagata^b, Nobutaka Kitamura^c, Ryushi Tazawa^a, Kazuhide Nakagaki^d, Koh Nakata^{a,*}

^a Bioscience Medical Research Center, Niigata University Medical and Dental Hospital, 1-754, Asahimachi-dori, Chuo-ku, Niigata 951-8510, Japan

^b Towa Environment Science Co., Ltd. Prophoenix Division, 1-24-22 Nanko-kita, Suminoe, Osaka 559-0034, Japan

^c Department of Medical Informatics, Niigata University Medical and Dental Hospital, 1-754, Asahimachi-dori, Chuo-ku, Niigata 951-8510, Japan

^d Laboratory of Infectious Diseases and Immunology, College of Veterinary Medicine, Nippon Veterinary and Life Science University, 1-1-5, Sendagi, Bunkyo-ku, Tokyo 113-8602, Japan

ARTICLE INFO

Article history:

Received 3 December 2013

Received in revised form 18 February 2014

Accepted 24 March 2014

Available online 9 May 2014

Keywords:

GM-CSF

TF-1 cells

CHO cells

Sialic acid

Oligosaccharide

ABSTRACT

To date, the biological activity of granulocyte macrophage-colony stimulating factor (GM-CSF) has been investigated by using mostly *Escherichia coli*- or yeast cell-derived recombinant human GM-CSF (erhGM-CSF and yrhGM-CSF, respectively). However, Chinese hamster ovary cell-derived recombinant human GM-CSF (crhGM-CSF), as well as natural human GM-CSF, is a distinct molecule that includes modifications by complicated oligosaccharide moieties. In the present study, we reevaluated the bioactivity of crhGM-CSF by comparing it with those of erhGM-CSF and yrhGM-CSF. The effect of short-term stimulation (0.5 h) on the activation of neutrophils/monocytes or peripheral blood mononuclear cells (PBMCs) by crhGM-CSF was lower than those with erhGM-CSF or yrhGM-CSF at low concentrations (under 60 pM). Intermediate-term stimulation (24 h) among the different rhGM-CSFs with respect to its effect on the activation of TF-1 cells, a GM-CSF-dependent cell line, or PBMCs was not significantly different. In contrast, the proliferation/survival of TF-1 cells or PBMCs after long-term stimulation (72–168 h) was higher at low concentrations of crhGM-CSF (15–30 pM) than that of cells treated with other GM-CSFs. The proportion of apoptotic TF-1 cells after incubation with crhGM-CSF for 72 h was lower than that of cells incubated with other rhGM-CSFs. These effects were attenuated by desialylation of crhGM-CSF. Clearance of crhGM-CSF but not desialylated-crhGM-CSF by both TF-1 cells and PBMCs was delayed compared with that of erhGM-CSF or yrhGM-CSF. These results suggest that sialylation of oligosaccharide moieties delayed the clearance of GM-CSF, thus eliciting increased long-term bioactivity *in vitro*.

© 2014 Elsevier Ltd. All rights reserved.

Abbreviations: ACN, acetonitrile; ANOVA, analysis of variance; CHO, Chinese hamster ovary; crhGM-CSF, CHO-derived recombinant human GM-CSF; erhGM-CSF, *Escherichia coli*-derived recombinant human GM-CSF; FCS, fetal calf serum; FITC, fluorescein isothiocyanate; GM-CSF, granulocyte macrophage-colony stimulating factor; JAK2, Janus kinase 2; MIP-1 α , macrophage inflammatory protein; NaN₃, sodium azide; PBMCs, peripheral blood mononuclear cells; SDS–PAGE, sodium dodecyl sulfate–polyacrylamide gel electrophoresis; STAT5, signal transduction and activator of transcription; TFA, trifluoroacetic acid; TOF mass spectrometer, time-of-flight mass spectrometer; yrhGM-CSF, yeast cell-derived recombinant human GM-CSF.

* Corresponding author. Tel.: +81 25 227 0847.

E-mail addresses: noiredge2007@yahoo.co.jp (A. Hashimoto), belltatnk@gmail.com (T. Tanaka), y-itoh@med.niigata-u.ac.jp (Y. Itoh), yamagata@prophoenix.jp (A. Yamagata), nktmr@m12.alpha-net.ne.jp (N. Kitamura), ryushi@med.niigata-u.ac.jp (R. Tazawa), nakagaki@nvlu.ac.jp (K. Nakagaki), radical@med.niigata-u.ac.jp (K. Nakata).

<http://dx.doi.org/10.1016/j.cyto.2014.03.009>

1043-4666/© 2014 Elsevier Ltd. All rights reserved.

1. Introduction

Granulocyte macrophage-colony stimulating factor (GM-CSF) is a hematopoietic growth factor that regulates the growth, differentiation, and maturation of myeloid precursor cells and promotes the function of mature neutrophils, eosinophils, and monocytes [1–4]. It elicits these diverse effects through interaction with a unique dodecameric receptor complex on cells, which consists of α and common β chains [5–7]. GM-CSF signaling induces phosphorylation of Janus kinase 2 (JAK2) and the common β chains, followed by activation of signal transducers and activators of transcription (STATs) [5,7,8]. Upon immune stimulation, it is produced by a variety of cell types, including T cells, macrophages, endothelial cells, and fibroblasts. Although GM-CSF is produced locally [3], it can

act in a paracrine fashion to recruit circulating neutrophils, monocytes, and lymphocytes to enhance their function in host defense [9,10]. GM-CSF is used clinically to prevent neutropenia and associated infections by promoting the proliferation of hematopoietic progenitor cells after chemotherapy, by promoting the differentiation of myeloid cells, and by enhancing the antibacterial activities of neutrophils and macrophages [10–14].

Natural human GM-CSF (hGM-CSF) has been purified from several sources, including medium conditioned with placenta cells or activated blood lymphocytes [15–19]. It is a glycoprotein that consists of 127 amino acid residues, with four cysteines involved in two disulfide bonds, forming a compact globular structure that comprises four α -helices joined by loops. It is found extracellularly as a homodimer [6,7] with two N-glycosylation sites at Asn27 and Asn37 and three O-glycosylation sites at Ser7, Ser9, and Thr10 [15]. The most heavily glycosylated hGM-CSF, with a molecular weight of 28–32 kDa, has two N-linked carbohydrate moieties, whereas the partially glycosylated hGM-CSF, with a molecular weight of 23–25 kDa, contains one N-linked carbohydrate moiety. A minimally glycosylated hGM-CSF with molecular weight of 16–18 kDa consists of only one O-linked carbohydrate [15,20].

Cells from various species can produce recombinant hGM-CSF (rhGM-CSF) [21,22]. However, only commercial preparations produced from *Escherichia coli* and *Saccharomyces cerevisiae* are available for clinical use. Commercial *E. coli*-derived recombinant hGM-CSF (erhGM-CSF), Molgramostim, is non-glycosylated, consists of 127 amino acid residues, has a molecular weight of 14.5 kDa, and is methylated at the N-terminal end [23]. Commercial *Saccharomyces*-derived recombinant hGM-CSF (yrhGM-CSF), Sargramostim, is a glycoprotein of 127 amino acids composed of three primary molecular species having molecular weights of 19.5, 16.8, and 15.5 kDa [23]. Its amino acid sequence differs from hGM-CSF by a substitution of leucine at position 23 [23]. On the other hand, rhGM-CSF derived from Chinese hamster ovary (CHO) cells (crhGM-CSF) has a molecular weight of 15–32 kDa with the same N-glycosylation and O-glycosylation sites as those of hGM-CSF, although the carbohydrate moieties added are probably different. Forno et al. demonstrated that the N-glycan terminal contains mono- and disialic acid residues, but has predominantly tri- or tetrasialic acid residues with and without N-acetylglucosamine repeat units. N-glycans contain more than 90% α -1,6-linked fucose at the proximal end [20].

The pattern of glycosylation on GM-CSF is known to affect its biological activity. Proliferation of a human monocytic leukemia cell line incubated with the heavily glycosylated hGM-CSF (28–32 kDa) was reduced six fold compared with proliferation after treatment with non-glycosylated erhGM-CSF, while neutrophil superoxide anion production was reduced by up to 10-fold. Partially glycosylated hGM-CSF (23–25 kDa) and minimally glycosylated hGM-CSF (16–18 kDa) have biological activity similar to that of erhGM-CSF. The binding capacity of these hGM-CSFs for the rhGM-CSF receptor on neutrophils decreases with increasing molecular weight [15]. Similarly, most studies on mammalian cell-derived, glycosylated GM-CSF (including crhGM-CSF) demonstrate that glycosylation of GM-CSF prolongs the *in vivo* half life by stabilizing the protein, but reduces its binding avidity to the GM-CSF receptor and decreases its biological activities such as colony-forming activity of bone marrow cells and neutrophil superoxide anion production [15,24].

In contrast to previous studies [15,24], we showed in the present study that glycosylated rhGM-CSF produced by CHO cells exhibited increased proliferation/survival of TF-1 cells, PBMCs and monocytes at low GM-CSF concentrations compared with that of erhGM-CSF and yrhGM-CSF *in vitro*. Desialylation of crhGM-CSF attenuated this effect, indicating that the sialyl residue is crucial for augmenting the long-term activity of GM-CSF. Moreover, we

examined the mechanism of this effect by measuring the clearance of rhGM-CSF by cells.

2. Materials and methods

2.1. Material

2.1.1. Cells

TF-1, a GM-CSF-dependent cell line, was kindly provided by Kitamura et al. [22].

Peripheral blood mononuclear cells (PBMCs) and monocytes were isolated from the peripheral blood of healthy donors as described previously [8]. Written informed consent was obtained under protocols approved by the institutional review boards of the Niigata University Medical Dental Hospital.

2.1.2. rhGM-CSF

Molgramostim and Sargramostim were purchased from Amoytop Biotech Co., Ltd. (Xiamen, Fujian, PRC) and Genzyme Corporation (Cambridge, MA, USA), respectively. crhGM-CSF was kindly provided by JCR Pharmaceuticals Co., Ltd. (Ashiya, Hyogo, Japan).

2.1.3. Desialylation of crhGM-CSF

crhGM-CSF (1 mg/ml) was incubated with neuraminidase agarose from *Clostridium perfringens* (0.05 U/ml, Sigma-Aldrich, MO, USA) in 100 mM sodium acetate buffer with CaCl_2 (pH 5.0) for 60 min at 37 °C. After the agarose was removed, the solution was dialyzed against PBS overnight at 4 °C.

2.2. Mass spectrometry

Protein (10 μ l) was mixed with 90 μ l of 0.1% trifluoroacetic acid (TFA) and 0.5 μ l of MB-HIC8 magnetic C8 beads (Bruker Daltonics, Hercules, MA, USA) in a PCR tube and then incubated for 5 min at room temperature. The tube was subsequently placed in a magnetic beads separator and the supernatant was removed by using a pipette. The magnetic beads were then washed three times with 100 μ l of 0.1% TFA. The bound proteins were eluted from the magnetic beads by using 4.5 μ l of 60% acetonitrile (ACN) in 0.1% TFA. Two microliters of the eluate was mixed with 1 μ l of matrix solution (10 g/l sinapinic acid in 70% ACN, 0.1% TFA) and was spotted on a polished steel plate. The mass spectra were obtained on an Ultraflex TOF/TOF mass spectrometer (Bruker Daltonics, Hercules, MA, USA) operated in positive-ion linear mode.

2.3. Phosphorylated STAT5 detection assay

Heparinized fresh whole blood was incubated with 15, 30, 60, or 500 pM rhGM-CSF, for 30 min at 37 °C and fixed, and then red blood cells were lysed in Fix/Lyse buffer (BD Biosciences, Franklin Lakes, New Jersey, USA) for 20 min at 37 °C. White blood cells were collected by centrifugation and fixed in ice-cold methanol at –20 °C for 1 h. After centrifugation, the cells were resuspended in 3% FCS/0.01% NaN_3 /PBS solution and incubated with Alexa Fluor 647-labeled anti-pSTAT5 (BD Biosciences, San Jose, CA, New Jersey, USA). Cells with phosphorylated STAT5 in granulocytes/monocytes detected by flow cytometry (Cell Analyzer, Sony, Tokyo, Japan).

2.4. Neutrophil CD11b stimulation index assay

The neutrophil CD11b assay was performed as described previously [25]. Aliquots of heparinized fresh whole blood were incubated with rhGM-CSF, and cell-surface CD11b levels were quantified by flow cytometry (Sony, Tokyo, Japan). The CD11b

stimulation index was calculated as the mean fluorescent intensity of stimulated neutrophils minus the mean fluorescent intensity of unstimulated neutrophils divided by the mean fluorescent intensity of unstimulated neutrophils and multiplied by 100.

2.5. Measurement of GM-CSF-induced MIP-1 α in PBMCs

To evaluate GM-CSF-induced MIP-1 α production in normal PBMCs, 1×10^6 cells were incubated with or without GM-CSF in macrophage-serum-free medium (GIBCO BRL, Palo Alto, CA, USA). MIP-1 α levels in the supernatant were measured by ELISA (Quantikine, R&D Systems, Mincapolis, MN, USA) according to the manufacturer's instructions [26].

2.6. Cell proliferation/survival assay

TF-1 cells, PBMCs and monocytes (2×10^4 cells/well) were incubated with various concentrations of GM-CSF in macrophage serum free medium (GIBCO BRL, Palo Alto, CA, USA) for 3 and 7 days, respectively [27]. At the end of the incubation, 10 μ l of 100 μ l (5-[2,4-bis(sodiooxysulfonyl)phenyl-3-(2-methoxy-4-nitrophenyl)-2-(4-nitrophenyl)-2H-tetrazole-3-ium]) CCK-8, Doujindo, Kumamoto, Japan) was added to each well. Cells were further incubated at 37 °C under 5% CO₂ for 4 h, and formazan formation was measured as absorbance at 450 nm by using a microplate reader (Bio-Rad, CA, USA).

2.7. Inhibition of TF-1 cell growth by antibodies

A cell proliferation/survival assay was performed in the presence or absence of 500 ng/ml goat anti-GM-CSF antibody (R&D Systems, Mincapolis, MN, USA), which was purified from the serum of a goat immunized with rhGM-CSF.

2.8. Morphology and cell-survival assay

TF-1 cells (1×10^5 cells) incubated with rhGM-CSF were cytocentrifuged at 200 rpm for 2 min by using a Cytospin (Thermo Scientific, Waltham, MA, USA) and were then stained with Diff-Quick (Sysmex, Hyogo, Japan). The sizes of five hundred cells were measured under a high magnification field by using a micrometer (MeCan Imaging, Saitama, Japan). The percentage of living cells was determined by flow cytometry (Sony, Tokyo, Japan) using staining with propidium iodide solution (Annexin-V-FLUOS Staining Kit, Roche, Basel, Switzerland) according to the manufacturer's instructions.

2.9. SDS-PAGE

rhGM-CSFs (6.5 ng) were subjected to SDS-PAGE under reducing conditions. The gel was stained by using gel stain solution (ORIOLE Fluorescent Gel Stain, Bio-Rad, CA, USA), and the banding pattern was visualized under an image analyzer (MiniLumi, Berthold Technologies, Bad Wildbad, Germany).

2.10. Detection of apoptosis

2.10.1. FITC-Annexin V preparation

TF-1 cells (1×10^6 cells) were stained with FITC-labeled anti-Annexin-V antibody (Annexin-V-FLUOS Staining Kit, Roche,

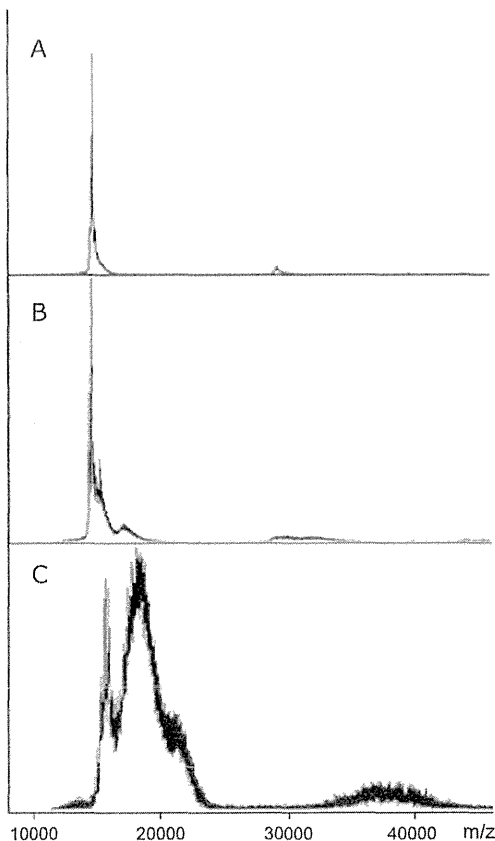


Fig. 1. Mass spectra of rhGM-CSFs. (A) *E. coli*-derived recombinant human GM-CSF. (B) Yeast-derived recombinant human GM-CSF. (C) CHO cell-derived recombinant human GM-CSF. The horizontal axis is the molecular weight (Da) and the vertical axis is the intensity.

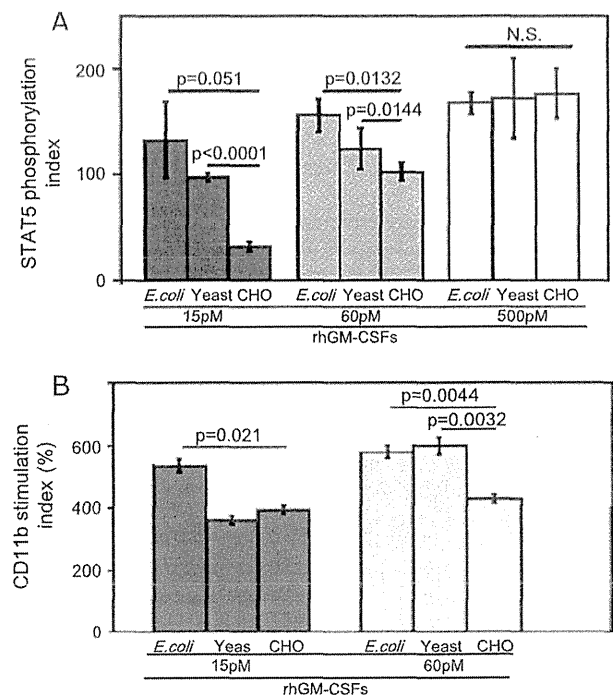


Fig. 2. Effect of short-term stimulation (0.5 h) by *E. coli*-, yeast-, and CHO cell-derived rhGM-CSF. The phosphorylation of STAT5 (A) and CD11b expression of neutrophils and monocytes (B). Whole blood cells were incubated for 0.5 h with 15, 60, or 500 pM of each rhGM-CSF for in (A) and 15 or 60 pM in (B). The vertical axis is STAT5 phosphorylation index (A) and CD11b stimulation index (B) is defined as described in Section 2.

Basel, Switzerland) for 15 min at 4 °C, and the stained cells were detected by flow cytometry (Sony, Tokyo, Japan). FITC-labeled mouse IgG isotype was used as the control.

2.10.2. DNA fragmentation assay

TF-1 cells (2×10^5 cells/ml) were incubated with 15 pM of rhGM-CSF for 3 days [27].

At the end of the incubation, DNA was extracted from TF-1 cells by using a QIAamp DNA Mini Kit (QIAGEN, Valencia, CA, USA). DNA (3.5 µg) was loaded on 1% agarose gel and electrophoresed for 25 min at 100 V (constant voltage). After the gel was stained with ethidium bromide solution (10 mg/ml, Nippon Gene, Tokyo, Japan), the banding pattern was visualized under an image analyzer (Mini-Lumi, Berthold Technologies, Bad Wildbad, Germany).

2.11. GM-CSF clearance assay

GM-CSF clearance assay was performed as described previously [8]. To assess receptor-mediated binding and uptake of exogenous GM-CSF, 1×10^6 PBMCs or 4×10^5 TF-1 cells per well in a 24-well culture plate were incubated in RPMI 1640 (GIBCO BRL, Palo Alto, CA, USA) containing 10% FCS (Nichirei, Bioscience Inc, Tokyo, Japan) 100 mg/ml streptomycin and 100 U/ml penicillin under 5% CO₂ at 37 °C. rhGM-CSF was added at concentrations of 5 and 15 pM to PBMCs and TF-1 cells, respectively. The concentration of rhGM-CSF in the supernatant of each well was then measured at 5, 10, 24, and 48 h by ELISA.

2.12. Statistical analysis

Numerical data were evaluated for normal distribution by using Shapiro–Wilk tests. Parametric data are presented as means (\pm SE). Parametric data were analyzed by using one-way factorial ANOVA measurements. Multiple comparisons were performed through a Bonferroni-adjusted *t*-test, with non-significance set at $p > 0.05$. All tests were two-sided and p values < 0.05 were considered statistically significant. Data were analyzed by using JMP (10.0.0) software (SAS, Cary, NC, USA).

3. Results

3.1. Molecular weight of rhGM-CSF

In this study, the bioactivity of rhGM-CSF derived from *E. coli*, yeast, and CHO cells was evaluated and compared. The mass spectrum of each GM-CSF shows distinct characteristic peaks: a single peak at 14.5 kDa for erhGM-CSF; peaks at 14.2, 14.4, and 15.0 kDa for yrhGM-CSF corresponding to a mean molecular weight of 14.7 kDa; and a number of peaks ranging from 16–28 kDa for crhGM-CSF corresponding to mean molecular weight of 19.0 kDa (Fig. 1A). The molar concentration of each rhGM-CSF was calculated from the original weight and volume, and then dividing by each mean molecular weight.

3.2. Short-term biological activity of rhGM-CSF

To compare the short-term bioactivity of the three rhGM-CSFs, we first evaluated the phosphorylation of STAT5 in monocytes and neutrophils stimulated for 0.5 h with the rhGM-CSFs. At both 15 and 60 pM rhGM-CSF, the percentage of pSTAT5-positive cells was significantly lower in crhGM-CSF-treated cells than in erhGM-CSF- or yrhGM-CSF-treated cells; whereas at 500 pM, this percentage was similar among the three rhGM-CSFs (Fig. 2A). Maximal values of CD11b stimulation indices at 60 pM of rhGM-CSF were $425 \pm 15\%$, $576 \pm 27\%$, and $625 \pm 33\%$, for crhGM-CSF,

erhGM-CSF, and yrhGM-CSF, respectively (Fig. 2B). These results indicate that the short-term effect of stimulation with crhGM-CSF was smaller than that with erhGM-CSF and yrhGM-CSF.

3.3. Intermediate-term biological activity of rhGM-CSF

When TF-1 cells were incubated with 30–120 pM rhGM-CSF for 24 h, the proliferation/survival was similar after treatment with crhGM-CSF, erhGM-CSF, and yrhGM-CSF (Fig. 3A). Likewise, MIP-1 α production in PBMCs was not different among the three rhGM-CSFs at both 15 and 500 pM (Fig. 3B).

3.4. Long-term biological activity of rhGM-CSF

We then investigated the long-term biological effect of GM-CSF on TF-1 cells, monocytes, and PBMCs incubated for 72, 168, and 168 h, respectively. The effect on the proliferation/survival rate of TF-1 cells was significantly greater in cells incubated with 15 pM crhGM-CSF than that on cells incubated with the same concentration of erhGM-CSF or yrhGM-CSF. However, the effects were equivalent among the three rhGM-CSFs at 60 pM. The ED₅₀ of each rhGM-CSF was 21 and 24 pM for erhGM-CSF and yrhGM-CSF, respectively, whereas it was 3.9 pM for crhGM-CSF (Fig. 4A). When monocytes were incubated with the GM-CSFs, the proliferation/survival rate was higher at 4 pM crhGM-CSF than that of cells incubated with the same concentration of other GM-CSFs. The ED₅₀ was 10.7, 4.9, and 1.8 pM for erhGM-CSF, yrhGM-CSF, and crhGM-CSF, respectively (Fig. 4B). Similarly, the proliferation/survival rate of PBMCs was higher with 2–4 pM crhGM-CSF compared with that with other GM-CSFs (Fig. 4C). Proliferation/survival in the presence of goat anti-GM-CSF antibody was comparable, whereas the

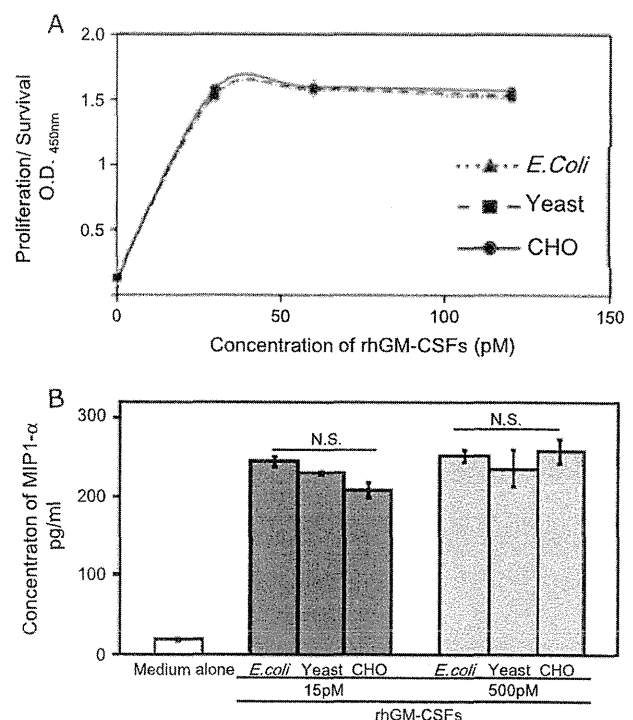


Fig. 3. Effect of intermediate-term stimulation (24 h) by rhGM-CSFs. (A) The proliferation/survival of TF-1 cells incubated for 24 h with various concentrations of rhGM-CSF derived from *E. coli* (N), yeast (J), and CHO (D) was measured by MTT assay, as described in Section 2. The vertical axis indicates formazan formation expressed as the OD at 450 nm. (B) MIP-1 α production of PBMCs incubated for 24 h with 0, 15, or 500 pM of *E. coli*, yeast-, and CHO-derived rhGM-CSF was measured by ELISA as described in Section 2.

inhibitory effect of the antibody was highest in crhGM-CSF. These data suggested that the effect of crhGM-CSF on the proliferation/survival of TF-1 cells was not due to oligosaccharide moieties but rather due to the GM-CSF peptide (Fig. 4D). After 3-day incubation with 30 pM erhGM-CSF, yrhGM-CSF, or crhGM-CSF, the number of viable TF-1 cells increased by multiples of 1.95 ± 0.5 , 2.0 ± 0.7 , and 6.45 ± 0.25 , respectively, compared with the number of viable cells before incubation (Fig. 4E). The size histogram of TF-1 cells incubated with crhGM-CSF displays a bimodal pattern with a mean value of $24.09 \mu\text{m}$, which is larger than that of erhGM-CSF-treated cells ($22.09 \mu\text{m}$) and yrhGM-CSF-treated cells ($22.0 \mu\text{m}$) (Fig. 4F). The viability of crhGM-CSF-stimulated TF-1 cells was significantly higher than that of TF-1 cells stimulated with other rhGM-CSFs. These results demonstrate that low concentrations of crhGM-CSF

not only promote proliferation/survival but also stimulate the growth of these cells more efficiently than do erhGM-CSF and yrhGM-CSF, and that the long-term effect of rhGM-CSF differs from the short- and intermediate-term outcomes. The long-term effects of erhGM-CSF and yrhGM-CSF for each condition were similar.

3.5. Modified bioactivity of crhGM-CSF after treatment with sialidase

To investigate the effect of sialyl residues located at the distal end of the oligosaccharide moieties [20] on cell proliferation/survival, we studied sialidase-treated crhGM-CSF. After treatment, mass spectrometry revealed a drastic reduction in the intensity of peaks corresponding to mono-, di-, tri-, and tetra-sialyl carbohydrates (Fig. 5A). This is also consistent with the banding pattern

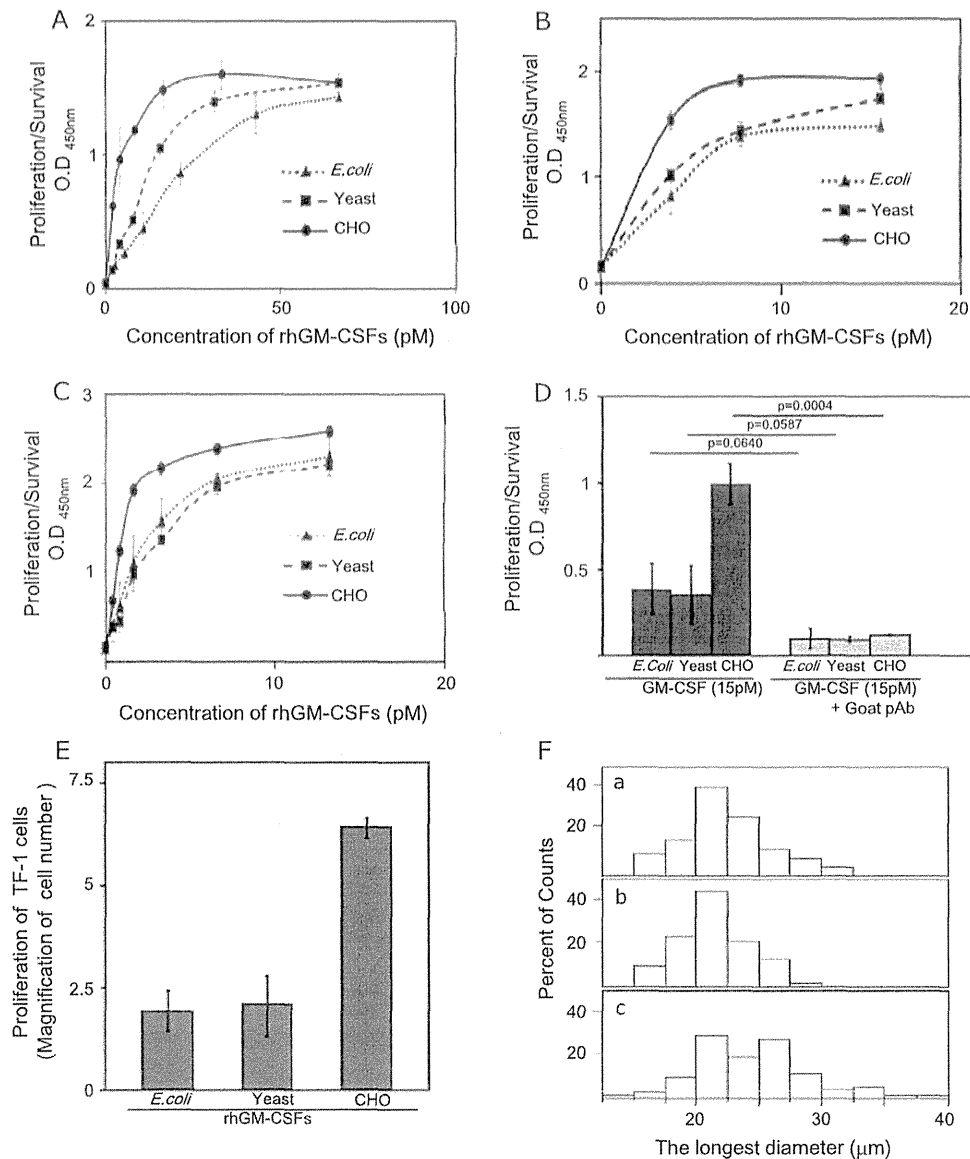


Fig. 4. Effect of long-term stimulation with various concentrations of rhGM-CSFs on the proliferation/survival of TF-1 cells, monocytes, and PBMCs. (A) Proliferation/survival of TF-1 cells incubated for 72 h with various concentrations (0–60 pM) of rhGM-CSF derived from *E. coli* (N), yeast (j), and CHO (d) was measured as described in Section 2. (B) Proliferation/survival of monocytes incubated for 168 h with various concentrations (0–15 pM) of rhGM-CSF derived from *E. coli* (N), yeast (j), and CHO (d) was measured as described in Section 2. (C) Proliferation/survival of PBMCs incubated for 168 h with various concentrations (0–15 pM) of rhGM-CSF derived from *E. coli* (N), yeast (j), and CHO (d) was measured as described in Section 2. (D) Effect of neutralizing goat anti-*E. coli*-derived GM-CSF antibody on the proliferation/survival of TF-1 cells incubated with 15 pM rhGM-CSFs. The vertical axis is the proliferation/survival of TF-1 cells (OD at 450 nm). (E) Magnification of proliferation was measured by enumerating viable TF-1 cells under a phase contrast microscopy before and after 72 h incubation with 30 pM rhGM-CSFs. (F) Size distribution of proliferation was measured by enumerating viable TF-1 cells under a phase contrast microscopy before and after 72 h incubation with 30 pM rhGM-CSFs. The horizontal axis is the largest diameter of cells and the vertical axis is the number of cells.

obtained by SDS–PAGE, in which several bands characteristic for crhGM-CSF are absent or weaker (Fig. 5B). Desialylation of crhGM-CSF markedly reduced the proliferation/survival rates to levels observed with erhGM-CSF- or yrhGM-CSF-treated cells (Fig. 5C). These results suggest that the up-regulated proliferation/survival induced by crhGM-CSF is likely due to its sialyl residues.

3.6. The effect of GM-CSF on apoptosis of TF-1 cells

The effect of GM-CSF on the apoptosis of TF-1 cells was evaluated by Annexin V expression with flow cytometry. When TF-1 cells were incubated with 30 pM crhGM-CSF for 3 days, 8.8% of the cells were apoptotic. In contrast, 17.0%, 21.4%, and 15.9% of cells were apoptotic upon incubation with erhGM-CSF, yrhGM-CSF, and sialidase-treated crhGM-CSF, respectively (Fig. 6A). TF-1 cells incubated with crhGM-CSF had fewer vacuolated nuclei and coagulated chromatin than those of cells incubated with other GM-CSFs (Fig. 6B). TF-1 cell apoptosis was also confirmed by DNA ladder formation via agarose gel electrophoresis (Fig. 6C). These results suggested that apoptotic TF-1 cells were less frequently observed in the presence of low concentration of crhGM-CSF than erhGM-CSF, yrhGM-CSF and sialidase-treated crh GM-CSF as TF-1 cells are GM-CSF dependent cell line. It is

plausible that GM-CSF bioactivity is likely to remain in culture supernatant of the cells incubated with crhGM-CSF compared with other rhGM-CSFs.

3.7. Clearance of rhGM-CSF by TF-1 cells and PBMCs

The clearance of crhGM-CSF by TF-1 cells and PBMCs was delayed compared with that of other GM-CSFs. After 24 and 48 h clearance assays, 13% and 9.5% of the initial crhGM-CSF concentration remained in the culture supernatant of PBMCs, whereas only 4.5% and 1.1% of erhGM-CSF, and 3.1%, 1% of yrhGM-CSF and 5.6% and 2.7% of sialidase-treated crhGM-CSF remained, respectively (Fig. 7A). On the other hand, after 24 and 48 h clearance assays, 7.5% and 3% of the initial crhGM-CSF concentration remained in the culture supernatant of TF-1 cells, whereas only 1.3% and 1.1% of erhGM-CSF, 1.1% and 1.0% of yrhGM-CSF and 2.9% and 2.7% of sialidase-treated crhGM-CSF remained, respectively (Fig. 7B). After 48 h incubation with erhGM-CSF, yrhGM-CSF, and sialidase treated crhGM-CSF, 15 pM of the same rhGM-CSF was except for crhGM-CSF added into each well. As shown in Fig. 7C, addition of each rhGM-CSF improved the proliferation/survival of TF-1 cells in the next 24 h reaching a similar level of those incubated with original 15 pM of crhGM-CSF for three days. Taken together with the data of proliferation/survival assay, it is likely that delayed clearance crhGM-CSF might prolong its biological activity *in vitro* (Fig. 7C).

4. Discussion

A number of studies have reported the expression of human GM-CSF by using natural or recombinant cells. These studies revealed that mammalian cells secrete GM-CSF proteins with variable molecular masses [20]. It has also been shown that its properties such as pharmacokinetics, binding affinity to the GM-CSF receptor, bioactivity, and immunogenicity are affected by glycosylation. In the present study, we demonstrated that compared with erhGM-CSF or yrhGM-CSF, crhGM-CSF promoted more efficiently the proliferation/survival of TF-1 cells, especially at low concentrations. In contrast to the results of the present study, natural hGM-CSF is thought to have lower biological activity with increasing glycosylation [15,24]. The pattern of glycosylation on GM-CSF has been found to affect its specific biological activity. Non-human expression systems such as yeast-, CHO cell-, or COS cell-derived rhGM-CSFs have distinct carbohydrate moieties and show different biological activities [18,28]. The half-life of hGM-CSF injected into rats decreases upon deglycosylation, indicating that the carbohydrate moieties influence the clearance, increase the stability, or alter the distribution of hGM-CSF. The carbohydrate structure of hematopoietic growth factors may therefore be important in determining their effective half-life *in vivo*. In this regard, we confirmed that *in vitro* GM-CSF clearance was also affected largely by the carbohydrate moieties of GM-CSF, especially its sialyl residues at the distal end of the oligosaccharide moieties.

The significance of the glycosylation of hematopoietic growth factors has been investigated previously. First, it is important for the secretion of glycoproteins. Erythropoietin secretion is prevented by site-directed mutagenesis of the N- or O-linked glycosylation sites [29–31]. As tunicamycin does not interfere with secretion of hGM-CSF, the N-linked carbohydrate is not crucial for this process [32]. Second, the N-linked carbohydrate influences the biological activity and receptor binding of other glycoprotein hormones and cytokines [29,33]. The *in vitro* activity of erythropoietin requires oligosaccharide moieties, but N-linked carbohydrates markedly reduce the *in vitro* activity of calcitonin. Glycosylation of luteinizing hormone is required for signal transduction, although

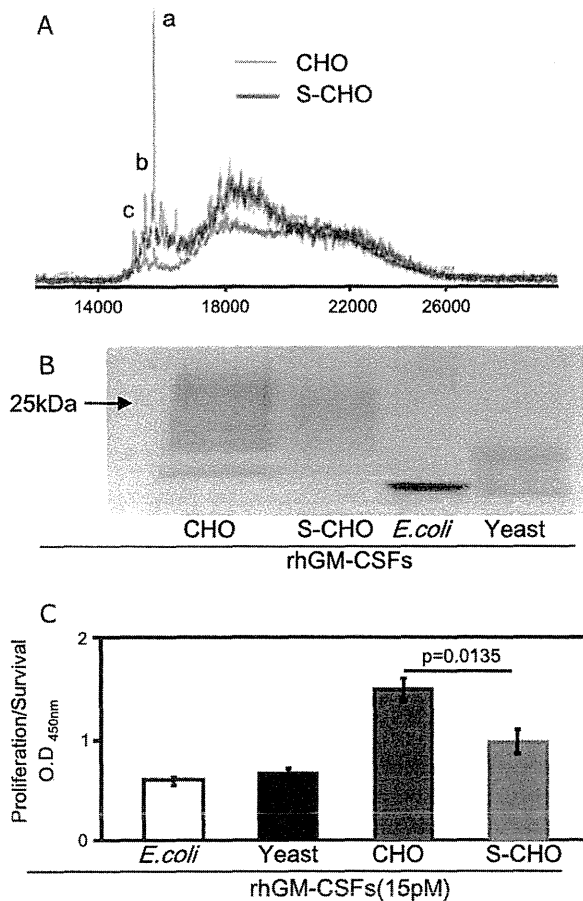


Fig. 5. Sialidase treatment of CHO-cell-derived rhGM-CSF and its biological activity. (A) Mass spectra of CHO cell-derived rhGM-CSF before (blue line) and after (red line) treatment with sialidase. (B) SDS-PAGE appearance of CHO cell-derived GM-CSF, CHO cell-derived GM-CSF after sialidase treatment, *E. coli*-derived GM-CSF, and yeast-derived GM-CSF. (C) The effect of sialidase treatment on the proliferation/survival of TF-1 cells after 72 h incubation with *E. coli*-, yeast-, CHO cells-derived rhGM-CSF or CHO cells-derived rhGM-CSF after sialidase treatment.

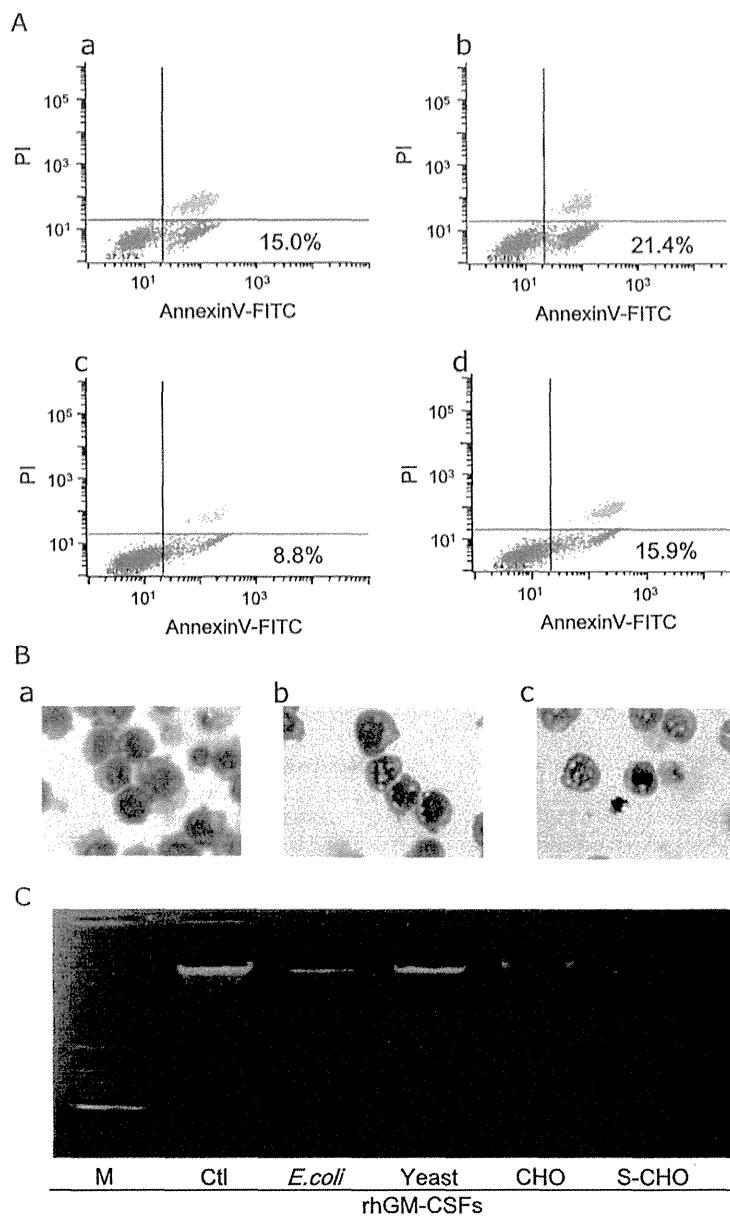


Fig. 6. Apoptosis of TF-1 cells incubated with 30 pM rhGM-CSFs for 72 h. (A) Flow cytometry results for apoptotic TF-1 cells incubated with rhGM-CSF derived from *E. coli* (a), yeast (b), CHO cells (c), or sialidase-treated CHO cells (d). The horizontal axis is the fluorescence intensity of Annexin V-FITC and the vertical axis is the fluorescence intensity of propidium iodide. (B) Morphology of TF-1 cells incubated with GM-CSF derived from CHO cells (a), yeast (b), and *E. coli* (c) at high magnification (1000 \times). Cells were cytocentrifuged and stained with Diff-Quick stain. (C) Agarose gel electropherogram of DNA extracted from TF-1 cells incubated with *E. coli*-, yeast-, CHO cells-derived rhGM-CSF or CHO cells-derived rhGM-CSF after sialidase treatment.

deglycosylated luteinizing hormone has higher receptor binding affinity [33]. Similarly, deglycosylation of hGM-CSF increases the receptor binding affinity [15]. However, in contrast to hGM-CSF, the most active forms are heavily glycosylated in luteinizing hormone [32].

Sialyl residues on carbohydrates in rhGM-CSF are considered crucial to the upregulation of the proliferation/survival of TF-1 cells because desialylation remarkably reduces this effect. Various sialylated forms of GM-CSF are produced in various tissues of mice and confer different physicochemical characteristics to murine GM-CSF [34]. Molecular weights of GM-CSF purified from various organs range from 37 to 200 kDa [32]; thus, it is possible that the bioactivity of GM-CSF produced in different tissues is regulated by the degree of sialylation. Since sialyl residues at the distal end of oligosaccharides can affect the specific activity of hGM-CSF as

well as its isoelectric points and affinities to the GM-CSF receptor, sialylation may alter the activity of hGM-CSF in a tissue-specific manner. The aforementioned studies are clinically important because therapy using hGM-CSF has been associated with side effects, which may relate to its activities as a mediator of inflammation rather than to its function as a growth factor [15]. If different glycosylation patterns allow hGM-CSF activity to be regulated, manipulation of the carbohydrate moieties may enable reduction of the inflammatory mediator effects of hGM-CSF without affecting the stimulation of myeloid cell production.

GM-CSF exerts its biological activities by binding to specific high-affinity cell-surface receptors. After binding, the ligand/receptor complex is rapidly internalized in most hematopoietic cells [35,36]. It is not fully known whether the turnover time of this internalization differs between different rhGM-CSFs. It is possible

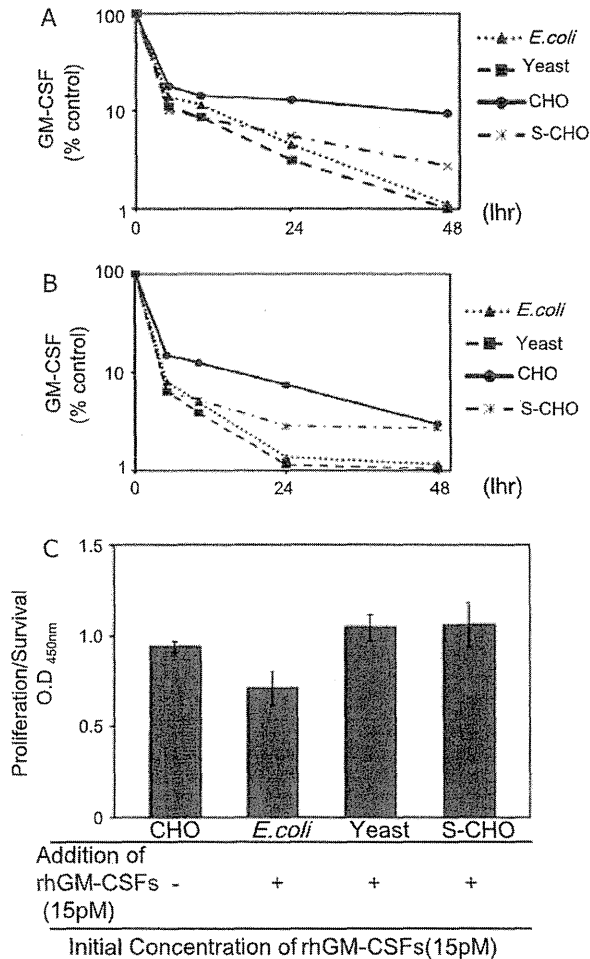


Fig. 7. GM-CSF clearance assay of TF-1 cells and peripheral blood mononuclear cells. (A) Peripheral blood mononuclear cells were incubated for 0–48 h with each 15 pM of *E. coli*-, yeast-, CHO cells-derived rhGM-CSF or CHO cells-derived rhGM-CSF after sialidase treatment. (B) TF-1 cells were incubated for 0–48 h with each 15 pM of *E. coli*-, yeast-, CHO cells-derived rhGM-CSF or CHO cells-derived rhGM-CSF after sialidase treatment. The horizontal axis is the time after the start of incubation. The vertical axis is percent each rhGM-CSF concentration per initial concentration at each time point in the culture supernatant. (C) After 48 h incubation with *E. coli*-, yeast-, CHO cells-derived rhGM-CSF or CHO cells-derived rhGM-CSF after sialidase treatment, 15 pM of the same rhGM-CSF was added into each well. The vertical axis is the proliferation/survival of TF-1 cells (OD at 450 nm).

that the oligosaccharide sialyl residue of crhGM-CSF can attenuate its binding to the low-affinity rhGM-CSF receptor α and/or associate with the rhGM-CSF β chain, resulting in downregulation of signal transduction and delayed clearance of the molecule [15]. The present study revealed that stimulation with low concentrations of crhGM-CSF augmented STAT5 phosphorylation less effectively than did low concentrations of erhGM-CSF and yrhGM-CSF. The sialyl residue may prolong the turnover cycle (known to be 40 s for erhGM-CSF) and thus maintain rhGM-CSF bioactivity for a longer period [35]. In the future, it is necessary to determine whether the sialyl residues of GM-CSF attenuate its binding to low-affinity receptors on hematopoietic cells or delay the process of its internalization into cells.

5. Conclusion

We have demonstrated for the first time that sialylated oligosaccharide moieties prolong the proliferation/survival of rhGM-CSF *in vitro*. Further studies are warranted to determine

the correlation of the oligosaccharide structure of crhGM-CSF with both signal transduction and internalization.

Authorship

A. Hashimoto and K. Nakata wrote the manuscript and designed the project.

A. Hashimoto performed experiments. Y. Ito and A. Yamagata assisted technical issues. T. Tanaka and N. Kitamura contributed to the statistical analysis of data. R. Tazawa participated in preparation of materials. K. Nakagaki provided variable information for methods. All authors read and approved the final manuscript.

Disclosure

The authors declare that they have no competing interests.

Acknowledgments

The authors thank JCR Pharmaceuticals Co., Ltd. for providing valuable information on recombinant Chinese hamster ovary cell derived GM-CSF. We also thank Takuji Suzuki, Kiyoko Akagawa, Tomoyuki Kawase, Takahito Nei, Takuro Sakagami and Kanji Uchida for valuable discussions and critical review of this manuscript. We appreciate Maiko Higuchi for technical help and Marie Mori for assistance of manuscript submission.

References

- [1] Atkinson YH, Lopez AF, Marasco WA, Lucas CM, Wong CG, Burns GF, et al. Recombinant human granulocyte-macrophage colony-stimulating factor (rh GM-CSF) regulates f Met-Leu-Phe receptors on human neutrophils. *Immunology* 1988;64:519–25.
- [2] Burgess AW, Begley CG, Johnson GR, Lopez AF, Williamson DJ, Mermod JJ, et al. Purification and properties of bacterially synthesized human granulocyte-macrophage colony stimulating factor. *Blood* 1987;69:43–51.
- [3] Metcalf D. Hematopoietic cytokines. *Blood* 2008;111:485–91.
- [4] Esnault S, Malter JS. GM-CSF regulation in eosinophils. *Arch Immunol Ther Exp (Warsz)* 2002;50:121–30.
- [5] Guthridge MA, Stomski FC, Thomas D, Woodcock JM, Bagley CJ, Berndt MC, et al. Mechanism of activation of the GM-CSF, IL-3, and IL-5 family of receptors. *Stem Cells* 1998;16:301–13.
- [6] Hansen G, Hercus TR, McClure BJ, Stomski FC, Dottore M, Powell J, et al. The structure of the GM-CSF receptor complex reveals a distinct mode of cytokine receptor activation. *Cell* 2008;134:496–507.
- [7] Martinez-Moczygemba M, Huston DP. Biology of common beta receptor-signaling cytokines: IL-3, IL-5, and GM-CSF. *J Allergy Clin Immunol* 2003;112:653–65 [quiz 66].
- [8] Tanaka T, Motoi N, Tsuchihashi Y, Tazawa R, Kaneko C, Nei T, et al. Adult-onset hereditary pulmonary alveolar proteinosis caused by a single-base deletion in CSF2RB. *J Med Genet* 2011;48:205–9.
- [9] Hercus TR, Thomas D, Guthridge MA, Ekert PG, King-Scott J, Parker MW, et al. The granulocyte-macrophage colony-stimulating factor receptor: linking its structure to cell signaling and its role in disease. *Blood* 2009;114:1289–98.
- [10] Trapnell BC, Whitsett JA. Gm-CSF regulates pulmonary surfactant homeostasis and alveolar macrophage-mediated innate host defense. *Annu Rev Physiol* 2002;64:775–802.
- [11] Huang FF, Barnes PF, Feng Y, Donis R, Chronos ZC, Idell S, et al. GM-CSF in the lung protects against lethal influenza infection. *Am J Respir Crit Care Med* 2011;184:259–68.
- [12] Weisbart RH, Golde DW, Clark SC, Wong GG, Gasson JC. Human granulocyte-macrophage colony-stimulating factor is a neutrophil activator. *Nature* 1985;314:361–3.
- [13] Socinski MA, Cannistra SA, Sullivan R, Elias A, Antman K, Schnipper L, et al. Granulocyte-macrophage colony-stimulating factor induces the expression of the CD11b surface adhesion molecule on human granulocytes *in vivo*. *Blood* 1988;72:691–7.
- [14] Shibata Y, Berclaz PY, Chronos ZC, Yoshida M, Whitsett JA, Trapnell BC. GM-CSF regulates alveolar macrophage differentiation and innate immunity in the lung through PU.1. *Immunity* 2001;15:557–67.
- [15] Cebon J, Nicola N, Ward M, Gardner I, Dempsey P, Layton J, et al. Granulocyte-macrophage colony stimulating factor from human lymphocytes. The effect of glycosylation on receptor binding and biological activity. *J Biol Chem* 1990;265:4483–91.
- [16] Broudy VC, Kaushansky K, Segal GM, Harlan JM, Adamson JW. Tumor necrosis factor type alpha stimulates human endothelial cells to produce granulocyte/

- macrophage colony-stimulating factor. *Proc Natl Acad Sci USA* 1986;83:7467–71.
- [17] Fibbe WE, van Damme J, Billiau A, Voogt PJ, Duinkerken N, Kluck PM, et al. Interleukin-1 (22-K factor) induces release of granulocyte-macrophage colony-stimulating activity from human mononuclear phagocytes. *Blood* 1986;68:1316–21.
- [18] Lee F, Yokota T, Otsuka T, Gemmell L, Larson N, Luh J, et al. Isolation of cDNA for a human granulocyte-macrophage colony-stimulating factor by functional expression in mammalian cells. *Proc Natl Acad Sci USA* 1985;82:4360–4.
- [19] Gabrilove JL, Welte K, Harris P, Platzer E, Lu L, Levi E, et al. Pluripoietin alpha: a second human hematopoietic colony-stimulating factor produced by the human bladder carcinoma cell line 5637. *Proc Natl Acad Sci USA* 1986;83:2478–82.
- [20] Forno G, Bollati Fogolin M, Oggero M, Kratje R, Etcheverrigaray M, Conradt HS, et al. N- and O-linked carbohydrates and glycosylation site occupancy in recombinant human granulocyte-macrophage colony-stimulating factor secreted by a Chinese hamster ovary cell line. *Eur J Biochem* 2004;271:907–19.
- [21] Sieff CA. Hematopoietic growth factors. *J Clin Invest* 1987;79:1549–57.
- [22] Kitamura T, Tange T, Terasawa T, Chiba S, Kuwaki T, Miyagawa K, et al. Establishment and characterization of a unique human cell line that proliferates dependently on GM-CSF, IL-3, or erythropoietin. *J Cell Physiol* 1989;140:323–34.
- [23] Dorr RT. Clinical properties of yeast-derived versus *Escherichia coli*-derived granulocyte-macrophage colony-stimulating factor. *Clin Ther* 1993;15:19–29 [discussion 18].
- [24] Moonen P, Mermod JJ, Ernst JF, Hirschi M, DeLamarier JF. Increased biological activity of deglycosylated recombinant human granulocyte/macrophage colony-stimulating factor produced by yeast or animal cells. *Proc Natl Acad Sci USA* 1987;84:4428–31.
- [25] Uchida K, Nakata K, Suzuki T, Luisetti M, Watanabe M, Koch DE, et al. Granulocyte/macrophage-colony-stimulating factor autoantibodies and myeloid cell immune functions in healthy subjects. *Blood* 2009;113:2547–56.
- [26] Rosen LB, Freeman AF, Yang LM, Jutivorakool K, Olivier KN, Angkasekwinai N, et al. Anti-GM-CSF autoantibodies in patients with cryptococcal meningitis. *J Immunol* 2013;190:3959–66.
- [27] Uchida K, Beck DC, Yamamoto T, Berclaz PY, Abe S, Staudt MK, et al. GM-CSF autoantibodies and neutrophil dysfunction in pulmonary alveolar proteinosis. *N Engl J Med* 2007;356:567–79.
- [28] Nicola NA, Metcalf D, Johnson GR, Burgess AW. Separation of functionally distinct human granulocyte-macrophage colony-stimulating factors. *Blood* 1979;54:614–27.
- [29] Dube S, Fisher JW, Powell JS. Glycosylation at specific sites of erythropoietin is essential for biosynthesis, secretion, and biological function. *J Biol Chem* 1988;263:17516–21.
- [30] Teh SH, Fong MY, Mohamed Z. Expression and analysis of the glycosylation properties of recombinant human erythropoietin expressed in *Pichia pastoris*. *Genet Mol Biol* 2011;34:464–70.
- [31] Darling RJ, Kuchibhotla U, Glaesner W, Micanovic R, Witcher DR, Beals JM. Glycosylation of erythropoietin affects receptor binding kinetics: role of electrostatic interactions. *Biochemistry* 2002;41:14524–31.
- [32] Jonathan Cebon, Burgess Antony W. Glycosylation of human granulocyte-macrophage colony stimulating factor alters receptor binding and biological activity. *TIGG* 1991;3(12).
- [33] Sairam MR, Bhargavi GN. A role for glycosylation of the alpha subunit in transduction of biological signal in glycoprotein hormones. *Science* 1985;229:65–7.
- [34] Walker F, Burgess AW. Specific binding of radioiodinated granulocyte-macrophage colony-stimulating factor to hemopoietic cells. *Embo J* 1985;4:933–9.
- [35] Elliott MJ, Moss J, Dottore M, Park LS, Vadas MA, Lopez AF. Differential binding of IL-3 and GM-CSF to human monocytes. *Growth Factors* 1992;6:15–29.
- [36] Walker F, Burgess AW. Internalisation and recycling of the granulocyte-macrophage colony-stimulating factor (GM-CSF) receptor on a murine myelomonocytic leukemia. *J Cell Physiol* 1987;130:255–61.

RESEARCH ARTICLE

Open Access

Secondary pulmonary alveolar proteinosis complicating myelodysplastic syndrome results in worsening of prognosis: a retrospective cohort study in Japan

Haruyuki Ishii¹, John F Seymour², Ryushi Tazawa³, Yoshikazu Inoue⁴, Naoyuki Uchida⁵, Aya Nishida⁵, Yoshihito Kogure⁶, Takeshi Saraya¹, Keisuke Tomii⁷, Toshinori Takada⁸, Yuko Itoh³, Masayuki Hojo⁹, Toshio Ichiwata¹⁰, Hajime Goto¹ and Koh Nakata^{3*}

Abstract

Background: Secondary pulmonary alveolar proteinosis (sPAP) is a very rare lung disorder comprising approximately 10% of cases of acquired PAP. Hematological disorders are the most common underlying conditions of sPAP, of which 74% of cases demonstrate myelodysplastic syndrome (MDS). However, the impact of sPAP on the prognosis of underlying MDS remains unknown. The purpose of this study was to evaluate whether development of sPAP worsens the prognosis of MDS.

Methods: Thirty-one cases of sPAP and underlying MDS were retrospectively classified into mild and severe cases consisting of very low-/low-risk groups and intermediate-/high-/very high-risk groups at the time of diagnosis of MDS, according to the prognostic scoring system based on the World Health Organization classification. Next, we compared the characteristics, disease duration, cumulative survival, and prognostic factors of the groups.

Results: In contrast to previous reports on the prognosis of MDS, we found that the cumulative survival probability for mild MDS patients was similar to that in severe MDS patients. This is likely due to the poor prognosis of patients with mild MDS, whose 2-year survival rate was 46.2%. Notably, 75% and 62.5% of patients who died developed fatal infectious diseases and exacerbation of PAP, respectively, suggesting that the progression of PAP *per se* and/or PAP-associated infection contributed to poor prognosis. The use of corticosteroid therapy and a diffusing capacity of the lung for carbon monoxide of less than 44% were predictive of poor prognosis.

Conclusion: Development of sPAP during the course of MDS may be an important adverse risk factor in prognosis of patients with mild MDS.

Keywords: Proteinosis, Myelodysplastic syndrome, GM-CSF, WPSS, Secondary pulmonary alveolar proteinosis, MDS, PAP, Refractory anemia

* Correspondence: radical@med.niigata-u.ac.jp

³Bioscience Medical Research Center, Niigata University Medical & Dental Hospital, 1-754 Asahimachi-dori, Chuo-ku, Niigata 9518520, Japan
Full list of author information is available at the end of the article

Background

Pulmonary alveolar proteinosis (PAP), a rare disorder predominantly affecting the lungs, is characterized by accumulation of surfactant lipids and proteins in the alveoli and terminal bronchioles [1]. PAP is clinically classified into three distinct forms, namely, autoimmune, secondary, and congenital PAP [2]. Autoimmune PAP is associated with disruption of granulocyte/macrophage colony-stimulating factor (GM-CSF) signaling caused by high levels of GM-CSF autoantibody in the lungs [3]. Secondary PAP (sPAP) results from underlying diseases that presumably impair surfactant clearance because of abnormal numbers and functions of alveolar macrophages (AMs). Of the 40 cases of sPAP previously reported by our group [4], 88% (n = 35) involved hematological disorders as underlying diseases. The probability of survival at two years was 46% in cases with sPAP complicating hematological disorders. The median survival time for all cases including 17 patients who died within two years of the sPAP diagnosis was 16 months. Although myelodysplastic syndrome (MDS) is the most frequent underlying disease of sPAP (n = 26, 65%), little information is available on the prognostic impact of development of sPAP on patient outcome.

MDS, a group of clonal hematological stem-cell disorders with ineffective myeloid hematopoiesis and varying degrees of bone marrow failure, is associated with a significant risk of progression to acute myeloid leukemia (AML). Clinical manifestations are variable, from indolent conditions with near-normal life expectancy to forms that rapidly develop into AML [5]. Clarifying much of this heterogeneity, the World Health Organization (WHO) developed a classification of MDS based on the presence of unilineage or multilineage dysplasia, bone marrow blast cell count, and cytogenetic features: refractory anemia (RA), RA with ringed sideroblasts (RARS), refractory cytopenia with multilineage dysplasia (RCMD), RCMD with ringed sideroblasts (RCMD-RS), RA with excess of blasts-1 (RAEB-1), and RA with excess of blasts-2 (RAEB-2) [6]. In 2007, Malcovati *et al.* developed a new prognostic scoring system (WHO classification-based prognostic scoring system (WPSS)) according to WHO subgroup, karyotype, and transfusion requirement. Through this system, cases with MDS are classified into very low-, low-, intermediate-, high-, or very high-risk groups [7]. WPSS is a dynamic system that accurately predicts the survival and risk of leukemic evolution in MDS patients at any time during the course of their disease. This time-dependent system seems particularly useful for lower-risk patients and for implementing risk-adapted treatment strategies.

Given the validation of WPSS criteria as a prognostic indicator for the course of MDS, it is applicable in

prognosis evaluation of MDS complicated by PAP (MDS/sPAP). In the present study, we evaluated this issue for the first time and found that development of sPAP worsens the prognosis of patients with otherwise low-risk MDS.

Methods

Subjects

Thirty-one patients in Japan who were diagnosed with sPAP with underlying MDS from July 1999 to June 2013 were evaluated. We obtained agreement from all treating physicians for each identified case, according to the Guidelines for Epidemiological Studies by The Ministry of Health, Labour, and Welfare. This was a retrospective cohort study approved by the Ethical Board of Kyorin University (H23-085-01). Cases, part of which were reported previously, were identified retrospectively [8-18].

Diagnosis

Diagnosis of MDS was made according to the 2002 WHO criteria [6]. One patient with unclassified MDS, two patients with myelofibrosis, and two patients with 20% marrow blasts who were considered as having AML were excluded from the study. MDS with isolated chromosome 5 deletion (del(5q)) and marrow blasts of <5% were included. Next, the patients were classified into RA, RARS, RCMD, RAEB-1, and RAEB-2 groups. Karyotypes were classified by using the International System for Cytogenetic Nomenclature Criteria [19]. Diagnosis of PAP was based on the following criteria: 1. histopathological findings from specimens obtained by surgical biopsy or transbronchial lung biopsy, or milk-like appearance with typical cytological findings from bronchoalveolar lavage fluid (BALF); 2. typical high-resolution computed tomography (HRCT) findings for PAP, such as ground glass opacity, consolidation, and interlobular septal thickening; and 3. negative result for serum GM-CSF autoantibody.

Classification by WPSS

The WPSS score was calculated according to the method of Malcovati *et al.* [7]. The score was calculated from the data of WHO subgroups (RA/RARS/5q-, RCMD/RCMD-RS, RAEB-1, and RAEB-2), karyotype abnormalities categorized according to the International Prognostic Scoring System [20], and transfusion requirement. The same weight (score of ≥ 1) was assigned to each variable for WHO subgroup, karyotype, and transfusion requirement. Based on the score, patients were classified according to the following five risk groups: very low (score = 0), low (score = 1), intermediate (score = 2), high (score = 3 to 4), and very high (score = 5 to 6). Transfusion dependency was defined as having at least one

red blood cell (RBC) transfusion every eight weeks over a period of four months.

Statistical analysis

The cumulative probability of survival and risk of progression to leukemia were estimated by using the Kaplan–Meier method. Patients undergoing transplantation treatment were censored at the time of the procedure in order to exclude any potential source of bias due to differential treatment. Variable data were analyzed through Kaplan–Meier methods to estimate the cumulative probabilities of overall survival. The difference in the cumulative probabilities within subcategories of patients was compared by using two-sided log rank test. Survival analyze was performed using Cox proportional model with time-dependent covariates to assess the effect of the variables of interest on overall survival.

Numeric data were evaluated for normal distribution and for equal variance by using the Kolmogorov–Smirnov test and Levene’s median test, respectively. Nonparametric data are presented as medians. Categorical data are presented as a percentage of the total or numerically, as appropriate. Statistical comparisons of nonparametric data were compared through the Wilcoxon test. Comparisons of categorical data were made with chi-square or Fischer’s exact tests. All tests were two-sided. Statistical significance was indicated by p values of <0.05. Data were analyzed by using SPSS 17.0 software for Windows.

Results

From September 1999 to May 2013, we centrally analyzed for GM-CSF autoantibody in the sera of 619

Japanese cases that had been diagnosed as PAP. Of those cases, 561 were positive for the antibody and 58 were negative. In the cases negative for GM-CSF antibody, 51 demonstrated obvious underlying diseases such as hematological disorders, autoimmune diseases, and infectious diseases. As shown in Figure 1, hematological disorders were the most common underlying disease, 31 cases of which involved MDS. These cases were investigated retrospectively in this study.

Demographic data are shown in Table 1. Diagnosis of MDS was performed in accordance with WHO criteria; 19, 1, 5, 3, and 3 cases were RA, RARS, RCMD, RAEB-1, and RAEB-2, respectively. Karyotyping revealed 2 cases of “high-risks of g e, 24 cases of “intermediate-riskmediatef, and 5 cases of “low-risks disease. As previously reported [10], there was over-representation of trisomy 8, as it was present in 16 cases (51.6%). RBC transfusion dependency was observed in 11 cases.

PAP was diagnosed on the basis of the BALF and HRCT results in 23 cases and by surgical biopsy and HRCT in eight cases. In 23 cases, diagnosis of MDS was done before diagnosis of PAP, whereas eight cases were diagnosed simultaneously.

According to the WPSS, the cases were classified into 2, 11, 7, 9, and 2 cases of very low-, low-, intermediate-, high-, and very high-risk groups, respectively. For statistical analysis, very low-/low-risk groups and intermediate-/high-/very high-risk groups were categorized as “mild MDS” and “severe MDS” DSere iz, respectively (Table 1). There was no difference in sex and age at the diagnosis of MDS and in hemoglobin concentration, absolute neutrophil count, and platelet count between mild and severe MDS cases. Then, the median age at diagnosis of

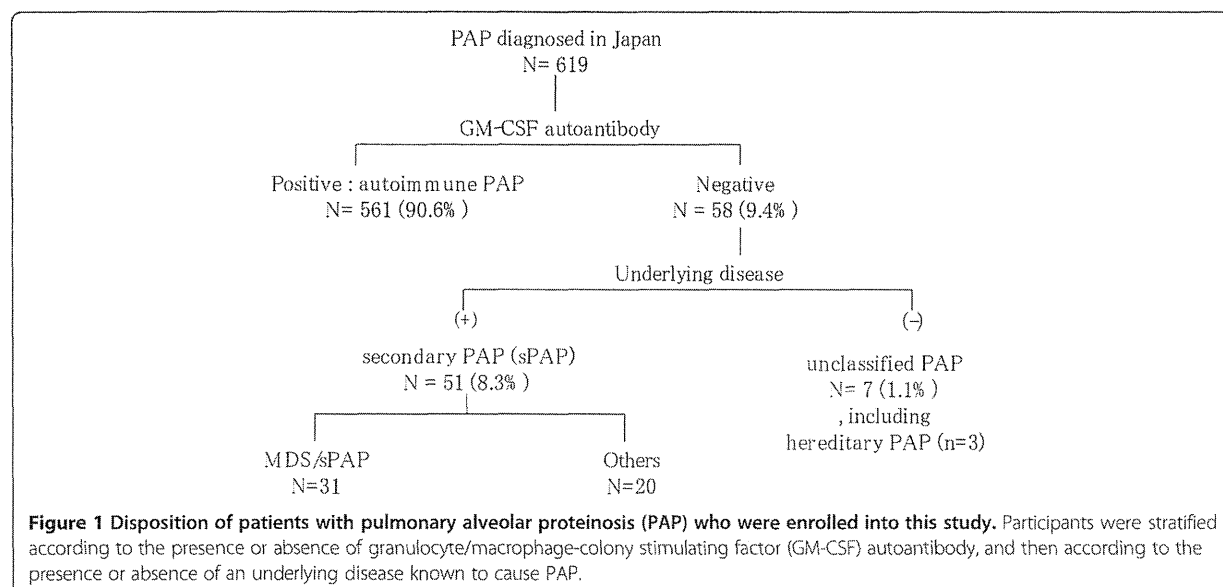


Table 1 Demographic data at diagnosis of MDS in each group classified according to the WPSS

Median (min.-max.)	Total (n = 31)	<WPSS risk groups>		p value
		<Very low + low >	<Inter - +high + very high>	
		Mild MDS (n = 13)	Severe MDS (n = 18)	
Sex (M/F)	19/12	7/6	12/6	0.71
Age at Dx of MDS	50 (27-75)	45 (30-67)	50 (27-75)	0.54
HbG (g/dl)	9.4 (4.8-16.4)	11.4 (5.5-16.4)	9.0 (4.8-13.9)	0.06
ANC (× 10 ⁹ /L)	1.84 (0.01-7.54)	1.46 (0.45-6.97)	2.74 (0.01-7.54)	0.68
PLT (× 10 ⁹ /L)	65 (6-219)	45 (14-219)	69 (6-196)	0.31
WHO subgroup: n (%)				
RA/RARS	20 (65)	13 (100)	7 (39)	<0.001
RCMD	5 (16)	0 (0)	5 (28)	0.058
RAEB-1,2	6 (19)	0 (0)	6 (33)	0.02
Karyotype*: n (%)				
Good type	2 (7)	2 (15)	0	0.16
Intermediate type	24 (77)	11 (85)	13 (72)	0.66
Poor type	5 (16)	0 (0)	5 (28)	0.058
RBC transfusion dependency**: n (%)	11 (35)	0 (0)	11 (61)	<0.001

(*). Cytogenetics was as follows. Good type: normal, -Y, del(5q), del(20q); poor type: complex (≥ three abnormalities), chromosome 7 anomalies; and intermediate type: other abnormalities.

(**) RBC transfusion dependency was defined as having at least one RBC transfusion every eight weeks over a period of four months. ANC, absolute neutrophil count; Dx, diagnosis; HbG, hemoglobin; MDS, myelodysplastic syndrome; PLT, platelets; RA, refractory anemia; RAEB, refractory anemia with blasts; RARS, refractory anemia with ringed sideroblasts; RBC, red blood cell; RCMD, refractory anemia with multilineage dysplasia; WHO, World Health Organization; WPSS, WHO classification-based prognostic scoring system.

Table 2 Clinical status at death (n = 17)

No.	WPSS at diagnosis	WHO criteria at diagnosis of MDS	AML progression	Progression of PAP	Pneumonia	
			6 (35.3%)	11 (64.7%)	11 (64.7%)	
Mild MDS	Very low + low	1			●	
		2		●		
		3	●		●	
		4		●	●	
		5	●			
		6		●		
		7		●		
Severe MDS	Intermediate	8			●	
		9		●	●	
		10		●	●	
		11	●	●	●	
		12	●		●	
		13		●		
	High + very high	14	RA		●	●
		15	RCMD	●	●	
		16	RAEB-1		●	●
		17	RAEB-2	●		●

AML, acute myeloid leukemia; MDS, myelodysplastic syndrome; PAP, pulmonary alveolar proteinosis; RA, refractory anemia; RAEB, refractory anemia with blasts; RCMD, refractory anemia with multilineage dysplasia; WHO, World Health Organization; WPSS, WHO classification-based prognostic scoring system.

MDS/sPAP was 51 years, and 84% of cases were symptomatic, with the most common symptoms being fever (45%), dyspnea on effort (42%), and cough (42%). The value of serum Krebs von den Lungen-6 (KL-6) and surfactant protein-D (SP-D) were elevated, and the diffusing capacities of the lung for carbon monoxide (% DLco) were very low in the absence of ventilation disorder in pulmonary function tests. There was no difference in the frequency of respiratory symptoms between patients with mild MDS and those with severe MDS. Serum biomarkers and pulmonary function tests showed no significant difference between the two groups.

Follow-up periods after diagnosis of MDS ranged from five to 254 months (median, 40 months) in all

patients (Additional file 1: Figure S1 and Additional file 2: Figure S2). During the follow-up period, 7 patients with mild MDS and 10 patients with severe MDS died, and 2 patients with mild MDS and 4 patients with severe MDS progressed to AML (Table 2). Two and five patients in the mild MDS and severe MDS groups, respectively, underwent transplantation therapies. They were censored at the time of the procedure. The duration from diagnosis of MDS to diagnosis of sPAP was variable, ranging from 0 to 168 months in the mild MDS group and from 0 to 228 months in the severe MDS group (Figure 2A). The median duration of MDS prior to diagnosis of sPAP in the mild MDS group was significantly longer than that in the severe MDS group

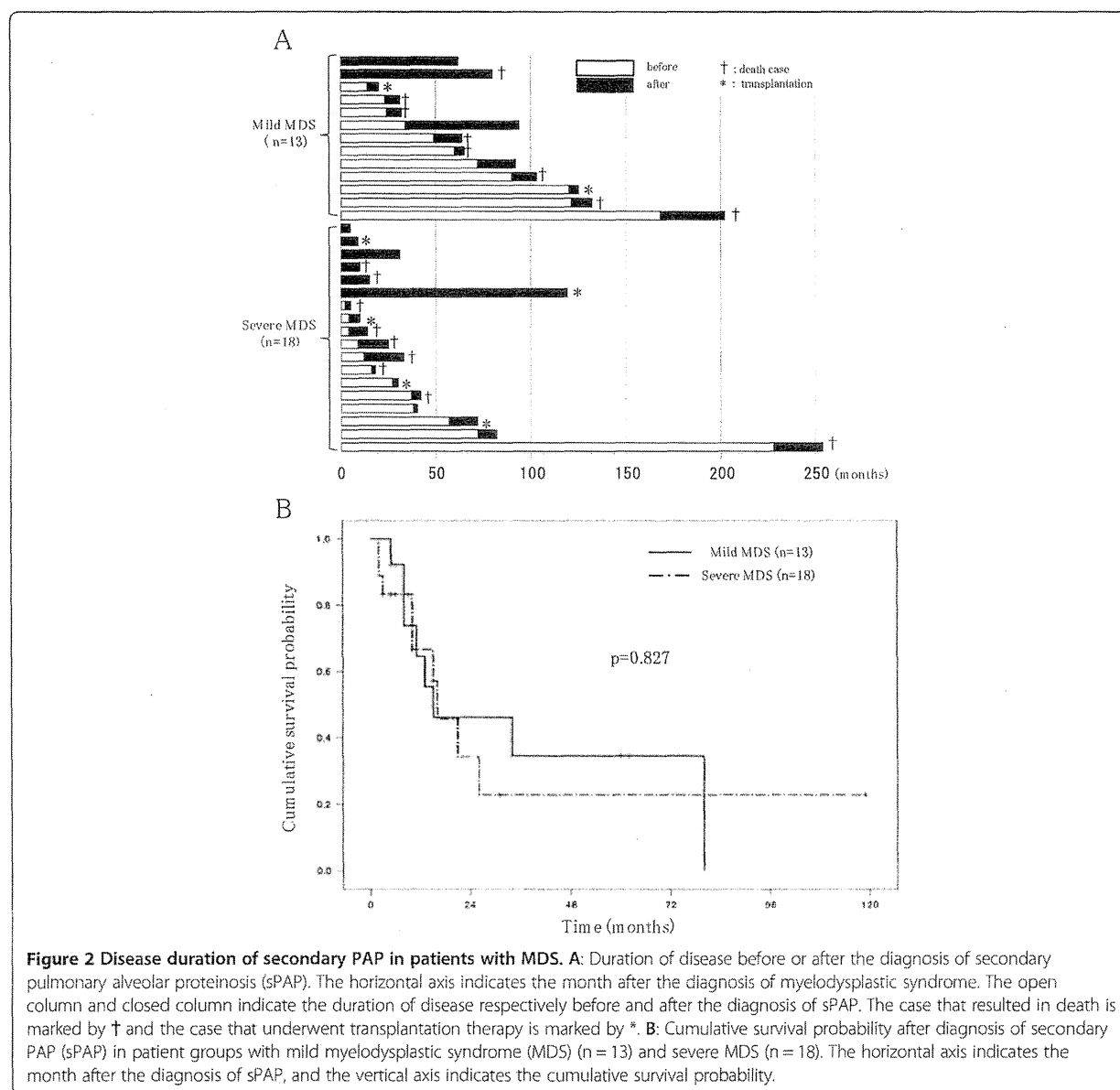


Figure 2 Disease duration of secondary PAP in patients with MDS. A: Duration of disease before or after the diagnosis of secondary pulmonary alveolar proteinosis (sPAP). The horizontal axis indicates the month after the diagnosis of myelodysplastic syndrome. The open column and closed column indicate the duration of disease respectively before and after the diagnosis of sPAP. The case that resulted in death is marked by † and the case that underwent transplantation therapy is marked by *. B: Cumulative survival probability after diagnosis of secondary PAP (sPAP) in patient groups with mild myelodysplastic syndrome (MDS) (n = 13) and severe MDS (n = 18). The horizontal axis indicates the month after the diagnosis of sPAP, and the vertical axis indicates the cumulative survival probability.

($p = 0.034$). Three patients in the mild MDS group and one in the severe MDS group survived for more than five years after diagnosis of sPAP. Of those, spontaneous remission of sPAP occurred in three cases.

A previous report [7] demonstrated that prediction of survival was dependent on the severity of MDS (as defined by WPSS) at any time of the disease. In contrast, patients with mild MDS in our study had cumulative survival probability similar to that of patients with severe MDS (Figure 2B, $p = 0.827$). This similarity may be due to poor prognosis of mild MDS after diagnosis of PAP. The cumulative survival probability curves of mild and severe MDS groups with median survivals of 13 and 15 months, respectively, are comparable. Concerning causes for the death of seven patients in the mild MDS group were progression to AML in two cases, PAP exacerbation in four cases, and fatal infectious disease in three cases (Table 2). Concerning causes for the death of

10 patients in the severe MDS group were progression to AML in 4 cases, PAP exacerbation in 7 cases, and fatal infectious disease in 8 cases. Fatal infectious diseases consistently arose from severe pneumonia with ($n = 4$) or without systemic sepsis, suggesting that progression of PAP was the major cause of death in both mild and severe MDS patients. These results suggest that occurrence of sPAP principally reduced the survival of patients with mild MDS. Pathogens isolated in the fatal cases were identified as *Aspergillus* species (four cases), *Pseudomonas aeruginosa* (four cases), and non-tuberculosis *Mycobacterium* species (four cases).

By performing univariate analysis using Cox proportional model we then searched for potential prognostic factors. Age, sex, respiratory symptoms, history of respiratory failure, diagnostic procedure for sPAP, and MDS group (mild or severe), were not associated with survival at the time of diagnosis of sPAP (Table 3). Treatment with

Table 3 Univariate analysis of overall survival after diagnosis of sPAP in MDS

Variable at diagnosis of sPAP	(n)	75% of OS (months)	50% of OS (months)	HR (95% CI)	P value
Age: 51 yrs or younger	16	8	16		
Older than 52 yrs	15	10	15	1.29 (0.48-3.41)	0.607
Gender: Male	19	10	16		
Female	12	11	21	1.12 (0.43-2.94)	0.804
MDS group: mild	13	10	15		
severe	18	11	16	1.11 (0.42-2.95)	0.830
Symptoms: (-)	5	26	26		
(+)	26	6	15	1.50 (0.33-6.65)	0.592
Dx procedure: Bronchoscopy	23	11	13		
Surgical biopsy	8	15	26	0.69 (0.23-2.04)	0.507
Respiratory failure: (-)	21	11	26		
(+)	10	5	10	2.18 (0.77-6.22)	0.142
Use of corticosteroid: (-)	16	16	80		
(+)	15	10	13	3.20 (1.09-9.38)	0.034
Serum KL-6 (U/ml): < 1960	16	13	26		
1960 ≤	15	5	15	1.52 (0.58-4.00)	0.389
Serum SP-D (ng/ml): < 147	15	10	26		
147 ≤	15	8	15	1.80 (0.62-5.22)	0.278
Serum SP-A (ng/ml): < 79	16	11	26		
79 ≤	14	5	15	2.79 (0.965-8.06)	0.058
%VC: 87 ≤	11	15	34		
< 87	11	8	15	3.27 (0.79-13.52)	0.101
FEV1%: 86 ≤	12	8	16		
< 86	10	13	34	0.52 (0.14-1.87)	0.322
%DLco: 44 ≤	9	21	34		
< 44	8	5	13	9.98 (1.03-96.11)	0.046

CI indicates confidence interval; OS, overall survival; DLco, diffusing capacity of the lung for carbon monoxide; Dx, diagnosis; FEV, forced expiratory volume; HR, hazard ratio; KL-6, krebs von den lungen-6; MDS, myelodysplastic syndrome; SP-A, surfactant protein -A; sPAP, secondary pulmonary alveolar proteinosis; SP-D, surfactant protein -D; VC, vital capacity.

corticosteroids was associated with poor survival ($p = 0.024$) (Figure 3A). However, the number of patients treated with steroid therapy did not differ between mild and severe MDS groups. A %DLco of <44% (Figure 3B) predicted poor prognosis ($p = 0.019$), whereas %vital capacity (%VC), forced expiratory volume (FEV) 1.0%, serum KL-6, SP-D, and surfactant protein-A (SP-A) did not.

Discussion

For the first time, we evaluated the prognosis of MDS/sPAP in a substantial cohort of patients, comparing mild

and severe MDS as classified according to WPSS criteria. Our data demonstrate that the duration from diagnosis of MDS to diagnosis of sPAP was longer in mild MDS than that in severe MDS, but the survival probability was similar after the diagnosis of sPAP regardless of MDS severity. As a whole, occurrence of PAP appeared to worsen the prognosis of patients with mild MDS. This result is supported by the fact that the major cause of death was not MDS-associated but rather sPAP-associated respiratory failure or infections. Prior to our report, 21 cases with MDS/sPAP have been reported

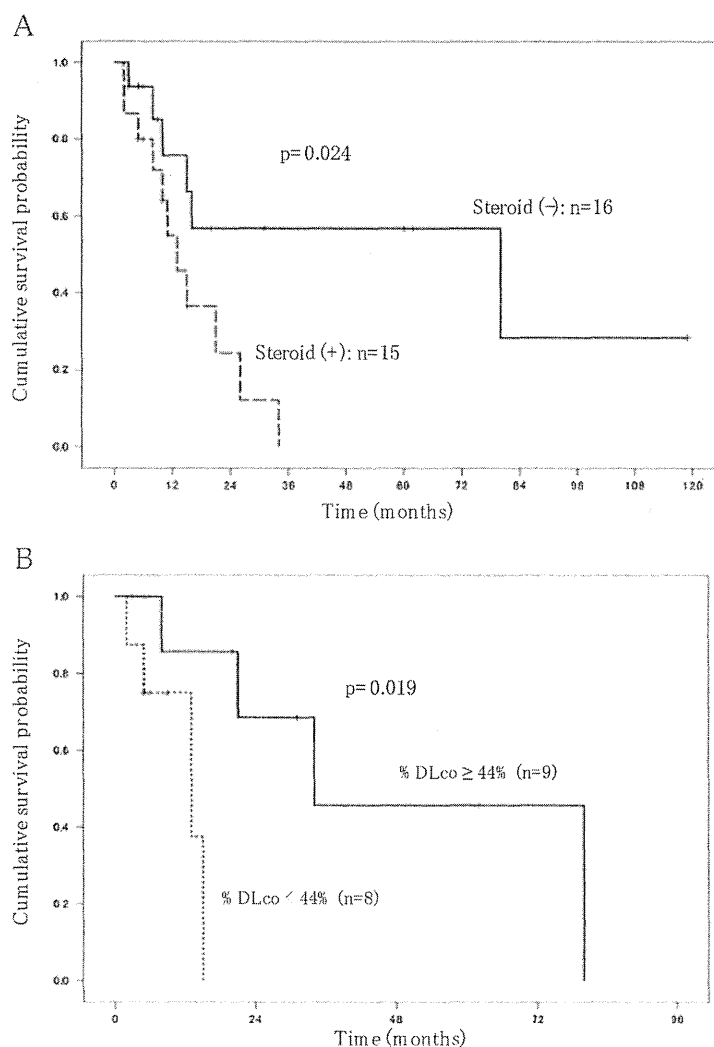


Figure 3 Risk factors for the prognosis of secondary PAP in patients with MDS. A: Cumulative survival probability after diagnosis of secondary PAP (sPAP) in myelodysplastic syndrome (MDS) cases with steroid therapy ($n = 15$) and in MDS cases without steroid therapy ($n = 16$). The horizontal axis indicates the month after the diagnosis of sPAP, and the vertical axis indicates the cumulative survival probability. The number of cases that received steroid therapy in the mild and severe MDS groups were six (46%) and nine (59%), respectively. **B:** Cumulative survival probability after diagnosis of secondary PAP (sPAP) in myelodysplastic syndrome (MDS) cases with diffusing capacity of the lung for carbon monoxide (%DLco) of <44% ($n = 8$) and in MDS cases with %DLco of >44% ($n = 9$). The horizontal axis indicates month after the diagnosis of sPAP, and the vertical axis indicates the cumulative survival probability.